Nonlinear Vibration of a Nonlocal Functionally Graded Beam on Fractional Visco-Pasternak Foundation

Nikola Nešić (✉ nikola.nesic@pr.ac.rs)
  Univerzitet u Pristini   https://orcid.org/0000-0001-6237-4735

Milan Cajić
  Swansea University College of Engineering

Danilo Karličić
  Mathematical Institute of the Serbian Academy of Sciences and Arts: Matematicki institut Srpske akademije nauka i umetnosti

Aleksandar Obradovic
  University of Belgrade Faculty of Mechanical Engineering: Univerziteta u Beogradu Fakultet Masinski

Julijana Simonović
  University of Niš: Univerzitet u Nisu

Research Article

Nonlinear vibration of a nonlocal functionally graded beam on fractional visco-Pasternak foundation

Nikola Nešić · Milan Cajić · Danilo Karličić · Aleksandar Obradović · Julijana Simonović

Abstract This paper investigates the nonlinear dynamic behavior of a nonlocal functionally graded Euler–Bernoulli beam resting on a fractional visco-Pasternak foundation and subjected to harmonic loads. The proposed model captures both, nonlocal parameter considering the elastic stress gradient field and a material length scale parameter considering the strain gradient stress field. Additionally, the von Karman strain-displacement relation is used to describe the nonlinear geometrical beam behavior. The power-law model is utilized to represent the material variations across the thickness direction of the functionally graded beam. The following steps are conducted in this research study. At first, the governing equation of motion is derived using Hamilton's principle and then reduced to the nonlinear fractional order differential equation through the single-mode Galerkin approximation. The methodology to determine steady-state amplitude-frequency responses via incremental harmonic balance method and continuation technique is presented. The obtained periodic solutions are verified against the perturbation multiple scales method for the weakly nonlinear case and numerical integration Newmark method in the case of strong nonlinearity. It has been shown that the application of the incremental harmonic balance method in the analysis of nonlocal strain gradient theory-based structures, can lead to more reliable studies for strongly nonlinear systems. In the parametric study is shown that, on one hand, parameters of the visco-Pasternak foundation and power-law index remarkable affect the response amplitudes. On the contrary, the nonlocal and the length scale parameters are having a small influence on the amplitude-frequency response. Finally, the effects of the fractional derivative order on the system's damping are displayed at time response diagrams and subsequently discussed.

Keywords Nonlocal strain gradient theory · Functionally graded beams · Fractional Pasternak layer · Duffing oscillator · Fractional damping · Incremental harmonic balance method

Nikola Nešić
Faculty of Technical Sciences, University of Priština, Kosovska Mitrovica, Serbia
E-mail: nikola.nesic@pr.ac.rs

Milan Cajić
College of Engineering, Swansea University, United Kingdom (*present address*)
Mathematical institute of the Serbian Academy of Sciences and Arts, Kneza Mihaila 36, Belgrade, Serbia
E-mail: mcajic@mi.sanu.ac.rs

Danilo Karličić
Mathematical institute of the Serbian Academy of Sciences and Arts, Kneza Mihaila 36, Belgrade, Serbia
E-mail: danilok@mi.sanu.ac.rs

Aleksandar Obradović
Faculty of Mechanical Engineering, University of Belgrade, Belgrade, Serbia
E-mail: aobradovic@mas.bg.ac.rs

Julijana Simonović
Faculty of Mechanical Engineering, University of Niš, Niš, Serbia
E-mail: julijana.simonovic@masfak.ni.ac.rs

1 Introduction

Structures with physical properties which are varied continuously and gradually along a certain direction are known as functionally graded (FG) materials [17, 38, 60]. The major advantage of such materials that are emphasized in the engineering practice is that they lack stress concentration, which is a common problem at interfaces of conventional laminated composites [17, 38]. FG materials are usually composed of two different material phases such as metal and ceramics. Despite a significant amount of work done in the field of FG structures, there is still a lot of space and need for the investigation of MEMS/NEMS systems based on FG

materials. Nanobeams and nanoplates are utilized in different MEMS/NEMS devices [48, 35], such as microactuators [44, 20], microswitches [70], micro sensors [42], nanoscale resonators [19], energy harvesting nanodevices [65], etc. For studying the dynamic behavior of such systems various approaches based on experiments, molecular dynamics simulations, and continuum mechanics are already employed in the literature [8, 14, 41, 28, 39, 52]. However, it can be time and skill-demanding to set up and validate the experiment or to implement molecular dynamics simulations for such structures. For these reasons, size-dependent continuum mechanics models gain popularity due to their simplicity in predicting the mechanical behavior of micro/nano-scaled structural systems. Various non-classical elasticity theories are used to capture the size effects in micro and nanostructures. Among them, the most vastly used continuum theories for studying the nanostructures are: nonlocal elasticity theory [52, 50, 47], strain gradient theory [28], modified couple stress theory (or modified strain gradient theory) [67], and the surface elasticity theory [62]. Some experiments [28] revealed that nonlocal elasticity theory shows limitations in displaying the stiffness-hardening effect. This deficiency can be avoided when nonlocal strain gradient theory (NLSGT) is used as originally described by Lim et al. [36], which includes both nonlocal and length scale effects into the consideration.

Many studies employed NLSGT when analyzing the mechanical behavior of FG structures. Gao et al. [15] investigated the nonlinear free vibration of FG circular nanotubes using NLSGT and two steps perturbation method. Janevski [23, 24] studied linear vibration, stability, and buckling of nonlocal strain gradient Euler-Bernoulli and Timoshenko beams under the influence of temperature. El-Borgi et al. [8] investigated the free and forced vibration response of a simply supported FG beam resting on the nonlinear elastic foundation. The authors applied the perturbation method of multiple scales to obtain the amplitude-frequency curves of the system. Other authors [21] studied the heat-induced nonlinear vibration of FG capacitive nanobeam within the framework of NLSGT. The semi-analytic perturbation method of averaging was applied to obtain the governing equations and study the steady-state responses. They also used a shooting technique in conjunction with the Floquet theory for capturing the periodic motions and examining their stability. Wang and Shen [63] investigated the lateral nonlinear vibration of an axially moving simply supported viscoelastic nanobeam based on NLSGT. They used a direct multiscale method to obtain the steady-state amplitude-frequency response in the subharmonic parametric resonance state as well as the Routh–Hurwitz criterion to determine the stability of the (non-) zero equilibrium solution. Jalaei et al. [22] investigated the dynamic stability of a temperature-dependent Timoshenko functionally graded nanobeam exposed to

the axial excitation load and magnetic field in a thermal environment. The authors used Navier's and Bolotin's method-based approach to solve the problem. Li et al. [32] studied the longitudinal vibration of rods also using the NLSGT and derived analytical solutions for predicting the natural frequencies and mode shapes for specified boundary conditions. They discovered that the NLSGT rod model exerts a stiffness-softening effect when the nonlocal parameter is larger than the length scale parameter and exerts a stiffness-hardening effect in the opposite case. Li [34] investigated the vibration of axially FG beams based on NLSGT and Euler-Bernoulli beam theory and solved the problem via the generalized differential quadrature method. Simsek [56] proposed a beam model for nonlinear free vibration of an FG nanobeam with immovable ends based on the NLSGT and Euler-Bernoulli (EB) beam theory in conjunction with the von-Karman's geometric nonlinearity. Liu [37] examined the nonlinear vibrational behavior of FG sandwich NLSGT nanobeams in the presence of initial geometric imperfection. Nonlinearity induced by the von Karman theory and a cosine function similar to the mode shape form is employed to describe the geometric imperfection mode. They used He's variational principle to solve a nonlinear differential equation and obtain nonlinear frequency. Based on NLSGT, Li and Hu [31] and Zhen and Zhou [73] studied the wave propagation in fluid-conveying viscoelastic single-walled carbon nanotubes. Moreover, Li [33] investigated the fluid critical flow velocities of fluid-conveying microtubes modeled using NLSGT and Timoshenko and Euler–Bernoulli beam theories.

Zhang et al. [71] studied the nonlinear dynamic response of a simply supported fractional viscoelastic beam subjected to transverse harmonic excitation. By using the averaging method, the authors obtained a steady-state response of a single-mode system. Numerical results are determined by an algorithm based on the fractional-order Grünwald–Letnikov derivative and verified with analytical results. Eyebe [13] investigated the nonlinear vibration of a nanobeam resting on a fractional-order Winkler-Pasternak foundation by using the D'Alembert principle to obtain the governing equations and a method of multiple scales to approximate the resulting nonlinear problem. Further, Lewandowski [29] investigated the nonlinear, steady-state vibration and stability of harmonically excited fractional viscoelastic beams. The viscoelastic material of the beams is described by using the Zener rheological model with fractional derivatives. Amplitude equations are obtained by using the finite element and the harmonic balance method in conjunction with the continuation method.

In the paper [5], a homogeneous Euler Bernoulli beam on a Winkler-type nonlinear, viscoelastic, and unilateral or bilateral foundation was considered. The presented model was subjected to multiple concentrated or distributed trans-

verse static or dynamic loads. The IHB method was suited for obtaining the nonlinear frequency response of the system. Obtained and presented amplitude-frequency diagrams were expectantly similar to diagrams from our study. However, the considered parameters set were different both regarding the loading and the foundation properties. Their interest was the reaction of the foundation, which models foam materials, both to compression and tension. Instead, we research the influence of the parameters of the fractional-order model of foundation that can represent a range of different materials from foams to rubbers. Furthermore, our numerical calculations were verified with two other numerical methods, namely with multiple time scales and Newmark methods.

In this work, a detailed investigation of the nonlinear vibration of the nonlocal strain gradient Euler-Bernoulli beam resting on the fractional visco-Pasternak foundation and subjected to harmonic loads is performed. The suggested model contains both, nonlocal parameter considering the nonlocal elastic stress field and a material length scale parameter considering the strain gradient stress field. The following steps are conducted in this research study. First, the governing equation of motion is derived using Hamilton's principle and then reduced to the nonlinear fractional order differential equation via Galerkin approximation. The methodology to determine steady-state amplitude-frequency responses via incremental harmonic balance method and continuation technique is presented. The obtained periodic solutions are verified against the perturbation multiple scales method and numerical integration Newmark method. At last, a detailed parametric study is performed to show the influence of power-law index, nonlocal parameter, length scale parameter, parameters of fractional visco-Pasternak foundation, and load factors on the amplitude-frequency response curves of the proposed nonlinear problem. Additionally, the effects of the fractional derivative order and power-law index on the system's damping are displayed at time response diagrams and subsequently discussed.

2 Preliminaries

2.1 Fractional derivative

The vibration of the deformable structures grounded on the different types of the foundation is present in a wide range of practical structures. Usually, the impact of the foundation layer has great importance and has to be modeled appropriately. The model of the foundation with different properties can be found in the literature [69]. Visco-Pasternak foundation model used in our study was upgraded with fractional-order time derivatives of the deformation function. This allows us to encompass the whole range of grounds with different properties. We will use the Riemann-Liouville definition (Eq.(1)) when considering the IHB and multiple scales solutions and the Grünwald–Letnikov definition (Eq.(2)) in the case of the Newmark method [49, 58]. The Riemann-Liouville definition is equal to Grünwald–Letnikov definition [49], and these two definitions are equivalent for a wide class of functions and are often used in real physical and engineering problems. For this reason, we can use one definition and then turn to another when calculating the frequency responses by approximate and numerical methods. Here, both definitions are given for clarity. The Riemann-Liouville fractional time derivative can be defined as left or right, and we will use the left one.

The left Riemann-Liouville derivative of the continuous and differentiable, on a time interval [a, b], function $f(t)$, is defined as:

$$_aD_t^\alpha f(t) = \frac{1}{\Gamma(n-\alpha)} \frac{d^n}{dt^n} \int_a^t \frac{f(\tau)}{(t-\tau)^{\alpha-n+1}} d\tau, \quad t \in [a,b],$$

(1)

where α is the fractional-order derivative parameter and $n \in N$ is a natural number such that $n-1 < \alpha < n$. To preserve the physicality of the structure, we limit our investigation to the case when fractional derivative order is $\alpha \in [0,1)$.

Grünwald–Letnikov definition of a fractional derivative is given as

$$_aD_t^\alpha f(t) = \lim_{h\to 0} \frac{_a\Delta_t^\alpha f(t)}{h^\alpha},$$

(2)

where

$$_a\Delta_t^\alpha f(t) = \sum_{j=0}^{[\frac{t-a}{h}]} (-1)^j \binom{\alpha}{j} f(t-jh),$$

(3)

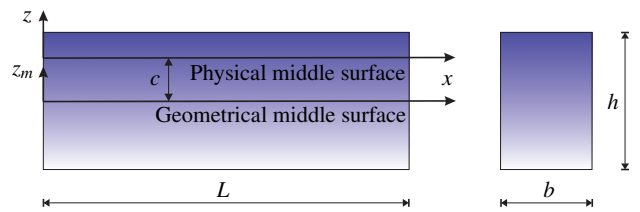and $[x]$ means the integer part of x.

Fig. 1: Coordinate systems in physical and geometrical middle surface.

2.2 Functionally graded material

A small-scale FG beam of width b and thickness h is made of two different materials, and the effective material properties (e.g. Young's modulus E and density ρ) vary continuously
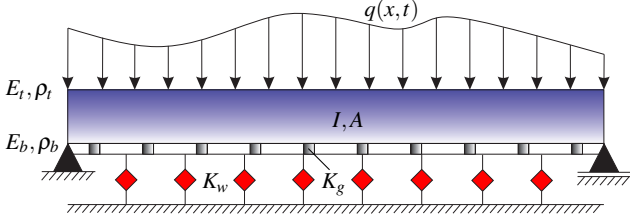
Fig. 2: Model of the nonlinear nonlocal strain gradient beam on a fractional visco-Pasternak foundation.

through the beam's thickness (z direction). Those materials properties regarding geometrical middle axis based on the power-law distribution function of material, are:

$$\mathscr{P}(z_m) = (\mathscr{P}_t - \mathscr{P}_b)\left(\frac{z_m}{h} + \frac{1}{2}\right)^k + \mathscr{P}_b, \tag{4}$$

where indices t and b denote the top and bottom layer of the beam and k is the power-law index, which determines the material variation in the thickness direction of the beam. Geometrical and physical middle surfaces of homogeneous materials coincide. However, the change of material properties in one direction shifts the physical middle surface from the geometrical one for some finite length c. Such new system of reference for FG materials and structures is proposed by several authors [3],[30], [56]. Therefore, to simplify the analysis and avoid the bending-stretching mode coupling effect we will use a new coordinate system where the x axis lies in the physical middle surface and the vertical axis is given as z, i.e.

$$z = z_m + c. \tag{5}$$

Constant c, denoting the position of the physical middle surface, can be calculated as

$$c = \frac{\int_{-\frac{h}{2}}^{\frac{h}{2}} z_m \mathscr{P}(z_m) dz_m}{\int_{-\frac{h}{2}}^{\frac{h}{2}} \mathscr{P}(z_m) dz_m}. \tag{6}$$
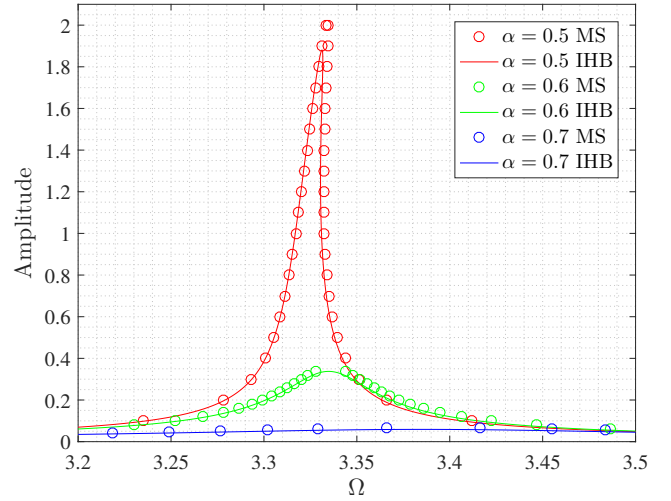
For our case of a rectangular FG beam with width b and height h, by substituting Eq.(4) in Eq.(6), expression for c is simplified to
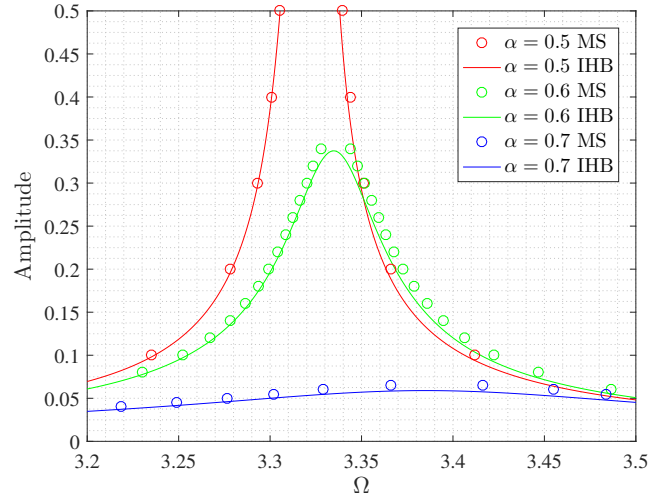
$$c = \frac{(E_t - E_b)hk}{2(2+k)(E_t + kE_b)}. \tag{7}$$

By taking the physical middle surface as a reference, material properties can be expressed as

$$E(z) = (E_t - E_b)\left(\frac{z}{h} + \frac{1}{2}\right)^k + E_b, \tag{8}$$

$$\rho(z) = (\rho_t - \rho_b)\left(\frac{z}{h} + \frac{1}{2}\right)^k + \rho_b. \tag{9}$$

(a)

(b)

Fig. 3: The amplitude-frequency response curves of the nonlinear nonlocal strain gradient FG beam on a fractional visco-Pasternak foundation are given in sub-figure (a). The sub-figure (b) is zoomed sub-figure (a). The periodic response is obtained by the incremental harmonic balance (IHB) method - solid line and multiple scales method - circles.

2.3 Nonlocal strain gradient theory

According to the nonlocal strain gradient theory [36], the strain energy U can be expressed as:

$$U = \frac{1}{2}\int_V (\sigma_{ij}\varepsilon_{ij} + \sigma_{ijk}^{(1)}\varepsilon_{ij,k})dV, \tag{10}$$

where σ_{ij} is the nonlocal stress, and $\sigma_{ijk}^{(1)}$ is the high-order nonlocal stress. Total stress is given by:

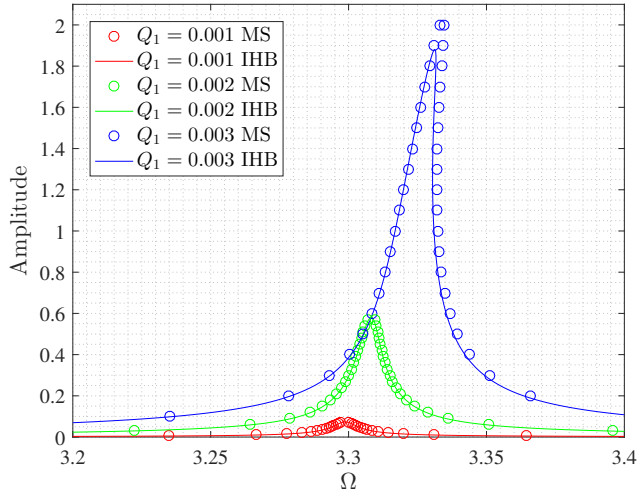$$t_{ij} = \sigma_{ij} - \nabla\sigma_{ijk}^{(1)}. \tag{11}$$

Fig. 4: The amplitude-frequency response curves of the nonlinear nonlocal strain gradient FG beam on a fractional visco-Pasternak foundation. The periodic response is obtained by the incremental harmonic balance (IHB) method - solid line and the multiple scales method - circles.

Constitutive equation for the nonlocal and local part [11] can be written as:

$$(1 - \mu^2 \nabla^2)\sigma_{xx} = E(z)\varepsilon_{xx}, \tag{12}$$

$$(1 - \mu^2 \nabla^2)\sigma_{xxx}^{(1)} = l^2 E(z)\varepsilon_{xx,x}, \tag{13}$$

where μ and l are the nonlocal and length scale parameter, respectively, $\nabla = \frac{\partial}{\partial x}$, $E(z)$ is the elasticity modulus, ε_{xx} is the axial strain, and $\varepsilon_{xx,x}$ is the axial strain gradient. The general nonlocal strain gradient constitutive relation is given as [32]:

$$(1 - \mu^2 \nabla^2)t_{xx} = (1 - l^2 \nabla^2)E(z)\varepsilon_{xx}. \tag{14}$$

Salehipour et al. [54] and later Batra [4] proposed the modified nonlocal theory that is applicable to non-homogenous materials. However, according to [54], when the Laplacian operator reduces to ($\nabla = \frac{\partial}{\partial x}$) and material properties of the beam are only the functions of the thickness coordinate z, then classical Eringen theory can be used to account for the small-scale effects in FG beams or plates. Moreover, by introducing the physical surface reference system one can avoid coupling between the bending and stretching modes. In our analysis, we adopted both assumptions to study the nonlinear dynamic response of the FG nonlocal beam resting on the fractional visco-Pasternak foundation.
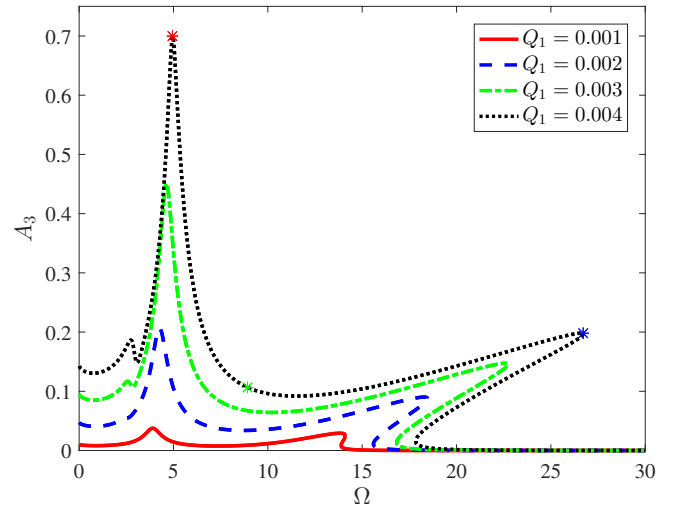
3 Beam model and equation of motion

Beam model is given in the Fig.(2). The displacement field of the Euler-Bernoulli beam is given as:

$$u_x(x,z,t) = u(x,t) - z\frac{\partial w}{\partial x}, \quad u_y(x,z,t) = 0, \quad u_z(x,z,t) = w(x,t),$$
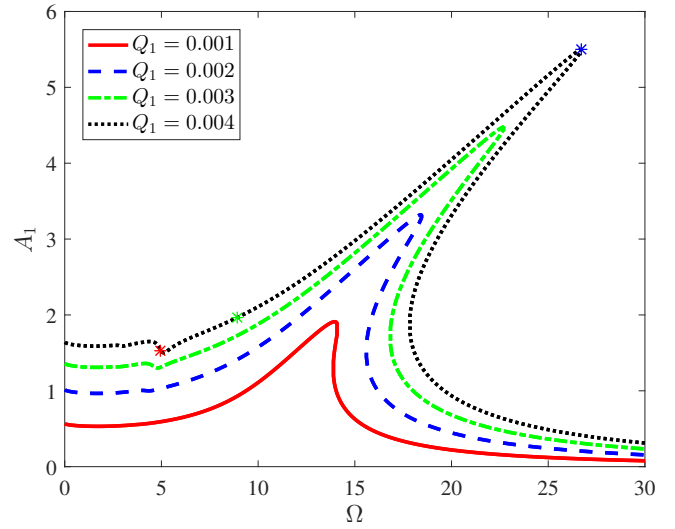
(a)

(b)

Fig. 5: The amplitude-frequency response curves A_1 - subfigure (a) and A_3 - sub-figure (b) of the nonlinear nonlocal strain gradient FG beam on fractional visco-Pasternak foundation of the amplitude Q_1.

$$\tag{15}$$

where u_x, u_y and u_z denote the displacements along the length, width and thickness directions, respectively. Terms u and w are the axial and transverse displacements of the physical middle surface, respectively. Thus, the non-zero strain components of Euler-Bernoulli beam with considered geometric nonlinearity takes the form

$$\varepsilon_{xx} = \frac{\partial u}{\partial x} + \frac{1}{2}\left(\frac{\partial w}{\partial x}\right)^2 - z\frac{\partial^2 w}{\partial x^2}. \tag{16}$$

We are considering the following stress resultants:

$$N_{xx} = \int_A t_{xx} dA, \quad N_{xx}^{(0)} = \int_A \sigma_{xx} dA, \quad N_{xx}^{(1)} = \int_A \sigma_{xx}^{(1)} dA,$$

$$M = \int_A z t_{xx} dA, \quad M^{(0)} = \int_A z\sigma_{xx} dA, \quad M^{(1)} = \int_A z\sigma_{xx}^{(1)} dA. \tag{17}$$

Further, we define the extensional A_{xx} and the bending coefficient D_{xx} as

$$\{A_{xx}, D_{xx}\} = b \int_{-\frac{h}{2}-c}^{\frac{h}{2}-c} \{1, z^2\} E(z) dz. \tag{18}$$

Note that for homogeneous beam $A_{xx} = EA$ and $D_{xx} = EI$. By substituting stress resultants Eq.(17) into Eq.(14), the axial force and moment are obtained as:

$$N_{xx} = N_{xx}^{(0)} - \frac{\partial N_{xx}^{(1)}}{\partial x}, \quad M = M^{(0)} - \frac{\partial M^{(1)}}{\partial x}. \tag{19}$$

By integrating the general constitutive relation Eq.(14) over area A, or multiplying it with z and integrating over area A, and using relations Eq.(18) and Eq.(17) leads to

$$N_{xx} = \mu^2 \frac{\partial^2 N_{xx}}{\partial x^2} + \left(1 - l^2 \frac{\partial^2}{\partial x^2}\right) A_{xx} \left(\frac{\partial u}{\partial x} + \frac{1}{2}\left(\frac{\partial w}{\partial x}\right)^2\right), \tag{20}$$

$$M = \mu^2 \frac{\partial^2 M}{\partial x^2} - D_{xx}\left(1 - l^2 \frac{\partial^2}{\partial x^2}\right)\frac{\partial^2 w}{\partial x^2}. \tag{21}$$

The variation of strain energy δU of the FG beam can be given as in [30, 57]:

$$\delta U = \int_V (\sigma_{xx}\delta\varepsilon_{xx} + \sigma_{xx}^{(1)}\nabla\delta\varepsilon_{xx})dV$$

$$= \int_0^L \left(N_{xx}\delta\frac{\partial u}{\partial x} + N_{xx}\frac{\partial w}{\partial x}\delta\frac{\partial w}{\partial x} - M\frac{\partial^2 w}{\partial x^2}\right)dx \tag{22}$$

$$+ \left[N_{xx}^{(1)}\delta\frac{\partial u}{\partial x} + N_{xx}^{(1)}\frac{\partial w}{\partial x}\delta\frac{\partial w}{\partial x} - M^{(1)}\frac{\partial^2 w}{\partial x^2}\right]_0^L.$$

Virtual kinetic energy considering both the longitudinal and transverse motions can be given by

$$\delta K = b \int_0^L \int_{-\frac{h}{2}-c}^{\frac{h}{2}-c} \rho(z)\frac{\partial u_x}{\partial t}\delta\frac{\partial u_x}{\partial t} dz dx$$

$$+ b \int_0^L \int_{-\frac{h}{2}-c}^{\frac{h}{2}-c} \rho(z)\frac{\partial u_z}{\partial t}\delta\frac{\partial u_z}{\partial t} dz dx \tag{23}$$

$$= \int_0^L m_0(\dot{u}\delta\dot{u} + \dot{w}\delta\dot{w})dx + \int_0^L m_2\frac{\partial\dot{w}}{\partial x}\delta\frac{\partial\dot{w}}{\partial x}dx.$$

Note that in Eq.(23) the mass moments of inertia takes the following form

$$\{m_0, m_1, m_2\} = b \int_{-\frac{h}{2}-c}^{\frac{h}{2}-c} \{1, z, z^2\}\rho(z)dz. \tag{24}$$
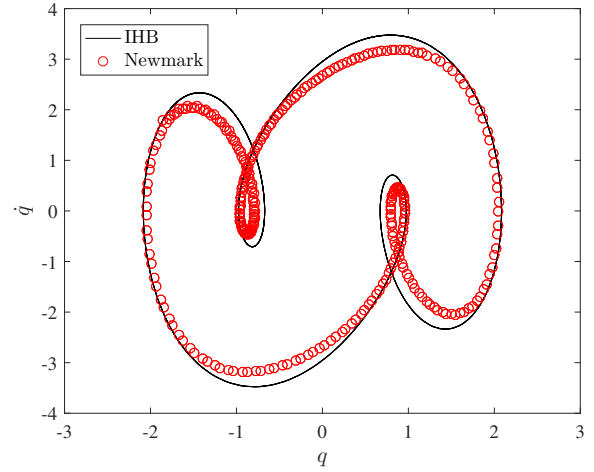
(a)
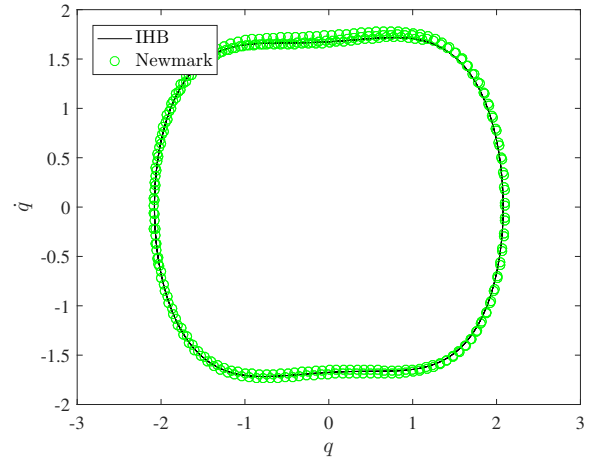
(b)

(c)

Fig. 6: The periodic response obtained by the incremental harmonic balance (IHB) method and Newmark method is taken for three different points in Fig.(5).

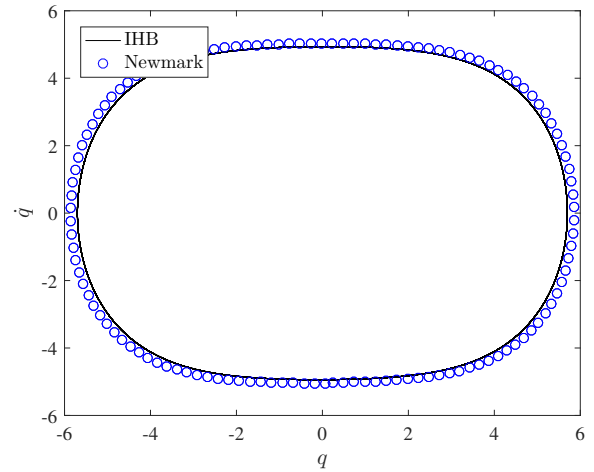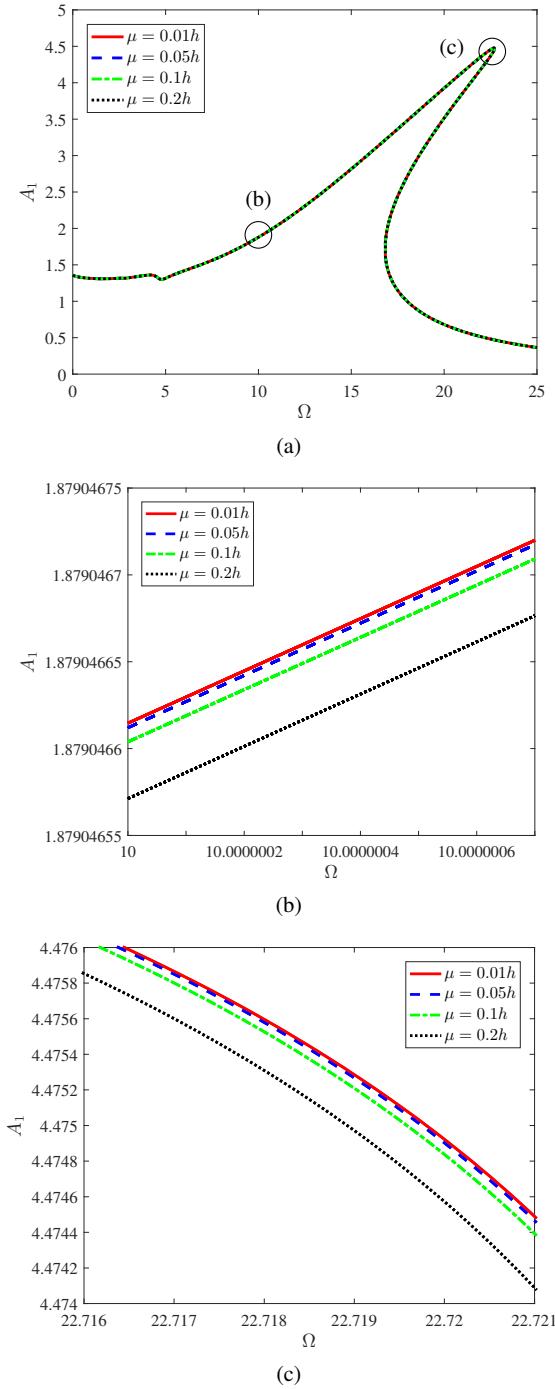Fig. 7: The amplitude-frequency response curves of the nonlinear nonlocal strain gradient FG beam on a fractional visco-Pasternak foundation in the first harmonic amplitude A_1 and different values of the nonlocal parameter μ are given in sub-figure (a). The periodic responses obtained by the incremental harmonic balance (IHB) method are taken far from the resonant state in sub-figure (b) and close to the resonant state in sub-figure (c).

Note that for homogeneous beam $m_0 = \rho A$ and $m_2 = \rho I$. According to Emam and Nayfeh [9], the first-order mass moment m_1 can be neglected in the virtual kinetic energy (Eq.(23)) since its contribution is relatively small.

Virtual work of external loads can be given by [2]:

$$\delta W = \int_0^L (F_m b + q)\delta w dx + \left[\overline{Q}\delta w - \overline{M}\delta \frac{\partial w}{\partial x} \right]_0^L, \qquad (25)$$

where

$$F_m = (k_w + K_w D^\alpha)w - (k_g + K_g D^\alpha)\frac{\partial^2 w}{\partial x^2}, \qquad (26)$$
$$q = Q_0 + Q_1 cos\Omega_1 t.$$

In Eq.(25) F_m is the restoring force due to the visco Pasternak layer, q is the distributed transverse load, $\overline{Q}$ is the external shear force, and $\overline{M}$ is the external bending moment. In Eq.(26) D^α is the operator of Riemann–Liouville fractional derivative. In [53], a similar foundation type is introduced but without the fractional time derivatives.

Hamilton's principle will be applied by using the Eq.(27):

$$\int_{t_1}^{t_2}(\delta K - \delta U - \delta W)dt = 0. \qquad (27)$$

By substituting Eqs.(22),(23), and (25) into Eq.(27), the following two equations of motion are obtained

$$\frac{\partial N_{xx}}{\partial x} - m_0\frac{\partial^2 u}{\partial t^2} = 0, \qquad (28)$$

$$\frac{\partial^2 M}{\partial x^2} + \frac{\partial}{\partial x}\left(N_{xx}\frac{\partial w}{\partial x}\right) + m_2\frac{\partial^4 w}{\partial x^2 \partial t^2} - m_0\frac{\partial^2 w}{\partial t^2} - bF_m - q = 0, \qquad (29)$$

with classical boundary conditions at $x = 0$ or $x = L$:

$$N_{xx} \quad \text{or} \quad u,$$
$$\frac{\partial M}{\partial x} + \overline{Q} \quad \text{or} \quad w, \qquad (30)$$

and non-classical boundary conditions at $x = 0$ or $x = L$:

$$N_{xx}^{(1)} \quad \text{or} \quad \frac{\partial u}{\partial x},$$
$$M^{(1)} \quad \text{or} \quad \frac{\partial^2 w}{\partial x^2}. \qquad (31)$$

By assuming the fast dynamics, acceleration in the axial direction in Eq.(28) is negligible. Therefore $N_{xx} = C = const.$ Substituting Eqs.(14) and (16) into Eq. (17), the axial force N_{xx} can be written as

$$N_{xx} = \left(1 - l^2\frac{\partial^2}{\partial x^2}\right)A_{xx}\left[\frac{\partial u}{\partial x} + \frac{1}{2}\left(\frac{\partial w}{\partial x}\right)^2\right]. \qquad (32)$$

By substituting Eq.(32) into Eq.(19) one can obtain

$$N_{xx}^{(0)} - \frac{\partial N_{xx}^{(1)}}{\partial x} = \left(1 - l^2 \frac{\partial^2}{\partial x^2}\right) A_{xx} \left[\frac{\partial u}{\partial x} + \frac{1}{2}\left(\frac{\partial w}{\partial x}\right)^2\right], \quad (33)$$

where

$$N_{xx}^{(0)} = A_{xx}\left[\frac{\partial u}{\partial x} + \frac{1}{2}\left(\frac{\partial w}{\partial x}\right)^2\right], \quad (34)$$

and

$$N_{xx}^{(1)} = l^2 A_{xx}\left[\frac{\partial^2 u}{\partial x^2} + \frac{\partial w}{\partial x}\frac{\partial^2 w}{\partial x^2}\right]. \quad (35)$$

In the case of hinged-hinged beams, the following boundary conditions are valid:

$$u(x=0) = 0, \quad N^{(1)}(x=0) = 0,$$
$$u(x=L) = 0, \quad N^{(1)}(x=L) = 0. \quad (36)$$

Substituting Eq.(34) into Eq.(32) and applying the boundary conditions Eq.(36), one can obtain expression for the axial force in the following form

$$N_{xx} = \frac{A_{xx}}{2L}\int_0^L \left(\frac{\partial w}{\partial x}\right)^2 dx. \quad (37)$$

Substituting Eq.(37) and the second equation of motion (29) into (21) moment M can be expressed as

$$M = \mu^2 \left[-\frac{A_{xx}}{2L}\int_0^L \left(\frac{\partial w}{\partial x}\right)^2 dx\frac{\partial^2 w}{\partial x^2} - m_2\frac{\partial^4 w}{\partial x^2 \partial t^2} + m_0\frac{\partial^2 w}{\partial t^2}\right.$$
$$\left. + bF_m + q\right] - D_{xx}\left(1 - l^2\nabla^2\right)\frac{\partial^2 w}{\partial x^2}. \quad (38)$$

Substituting Eq.(38) in (21), we obtain the size-dependent nonlinear equations of motion for an FG Euler-Bernoulli beam model based on the nonlocal strain gradient theory

$$\left(1 - \mu^2\nabla^2\right)\left[-\frac{A_{xx}}{2L}\int_0^L \left(\frac{\partial w}{\partial x}\right)^2 dx\frac{\partial^2 w}{\partial x^2}\right.$$
$$\left. - m_2\frac{\partial^4 w}{\partial x^2 \partial t^2} + m_0\frac{\partial^2 w}{\partial t^2} + bF_m + q\right]$$
$$+ D_{xx}\left(1 - l^2\nabla^2\right)\frac{\partial^4 w}{\partial x^4} = 0. \quad (39)$$

After substituting relations for the external loads (Eq.(26)) in Eq.(39), it leads to Eq.(40), given by

$$\left(1 - \mu^2\nabla^2\right)\left[-\frac{A_{xx}}{2L}\int_0^L \left(\frac{\partial w}{\partial x}\right)^2 dx\frac{\partial^2 w}{\partial x^2}\right.$$
$$- m_2\frac{\partial^4 w}{\partial x^2 \partial t^2} + m_0\frac{\partial^2 w}{\partial t^2} + bk_w w + bK_w D^\alpha w$$
$$\left. - bk_g\frac{\partial^2 w}{\partial x^2} - bK_g D^\alpha\frac{\partial^2 w}{\partial x^2} + Q_0 + Q_1 cos\Omega_1 t\right]$$
$$+ D_{xx}\left(1 - l^2\nabla^2\right)\frac{\partial^4 w}{\partial x^4} = 0. \quad (40)$$

We introduce the following nondimensional parameters:

$$\overline{X} = \frac{x}{L}, \quad \overline{W} = \frac{w}{k_x}, \quad \Sigma = \frac{l}{L}, \quad \lambda = \frac{\mu}{L}, \quad \zeta = \frac{b}{L}, \quad \tau = tS$$

$$\tau^\alpha = t^\alpha S^\alpha, \quad S = \frac{k_x}{L^2}\sqrt{\frac{A_{xx}}{m_0}} \quad y = \frac{m_2}{m_0 L^2}, \quad F_0 = \frac{Q_0 L^4}{A_{xx}k_x^3}$$

$$F_1 = \frac{Q_1 L^4}{A_{xx}k_x^3}, \quad \Omega = \Omega_1\frac{L^2}{k_x}\sqrt{\frac{m_0}{A_{xx}}}, \quad k_1 = \frac{\zeta k_w L^5}{A_{xx}k_x^2},$$

$$K_1 = \frac{\zeta K_w L^5}{A_{xx}k_x^2}S^\alpha, \quad k_2 = \frac{\zeta k_g L^3}{A_{xx}k_x^2}, \quad K_2 = \frac{\zeta K_g L^3}{A_{xx}k_x^2}S^\alpha. \quad (41)$$

Note that k_x, appearing in Eq.(41), is the radius of gyration, defined in Eq.(42) as

$$k_x = \sqrt{\frac{D_{xx}}{A_{xx}}}. \quad (42)$$

For the homogenous beam $k_x = \sqrt{\frac{I_x}{A}}$. Using nondimensional parameters from Eqs.(41) in Eq.(40) nonlinear equation of motion is transformed into the following nondimensional form

$$\left(1 - \lambda^2\frac{\partial^2}{\partial \overline{X}^2}\right)\left[-\frac{1}{2}\int_0^1 \left(\frac{\partial \overline{W}}{\partial \overline{X}}\right)^2 d\overline{X}\frac{\partial^2 \overline{W}}{\partial \overline{X}^2}\right.$$
$$- y\frac{\partial^4 \overline{W}}{\partial \overline{X}^2 \partial \tau^2} + \frac{\partial^2 \overline{W}}{\partial \tau^2} + k_1\overline{W} + K_1 D_\tau^\alpha\overline{W}$$
$$\left. - k_2\frac{\partial^2 \overline{W}}{\partial \overline{X}^2} - K_2 D_\tau^\alpha\frac{\partial^2 \overline{W}}{\partial \overline{X}^2} + F_0 + F_1\cos\Omega\tau\right]$$
$$+ \left(1 - \Sigma^2\frac{\partial^2}{\partial \overline{X}^2}\right)\frac{\partial^4 \overline{W}}{\partial \overline{X}^4} = 0. \quad (43)$$

The solution of Eq.(43) could be assumed as a sum of products of amplitude and time functions for each mode. The most usual is single-mode discretization which has been used by many authors (For example [8, 13, 16, 18, 21, 29, 32, 36, 53, 56, 61, 62]), and a solution would be assumed as in Eq.(44). In our case, this is legitimate, since we have only cubic nonlinearity, and Nayfeh and Lacarbonara have shown in their study [45] that in certain cases one-mode Galerkin approximation fails to predict the dynamic behavior of hinged-hinged beams, especially when quadratic type nonlinearity is involved and even modes are observed in certain subharmonic or superharmonic resonance conditions.

$$\overline{W}\left(\overline{X}, \tau\right) = \phi_n\left(\overline{X}\right)q(\tau), \quad (44)$$

where $\phi_n\left(\overline{X}\right)$ is the amplitude function, $q(\tau)$ is the time function and $n = 1, 2, ...$ is the mode number. Coefficients
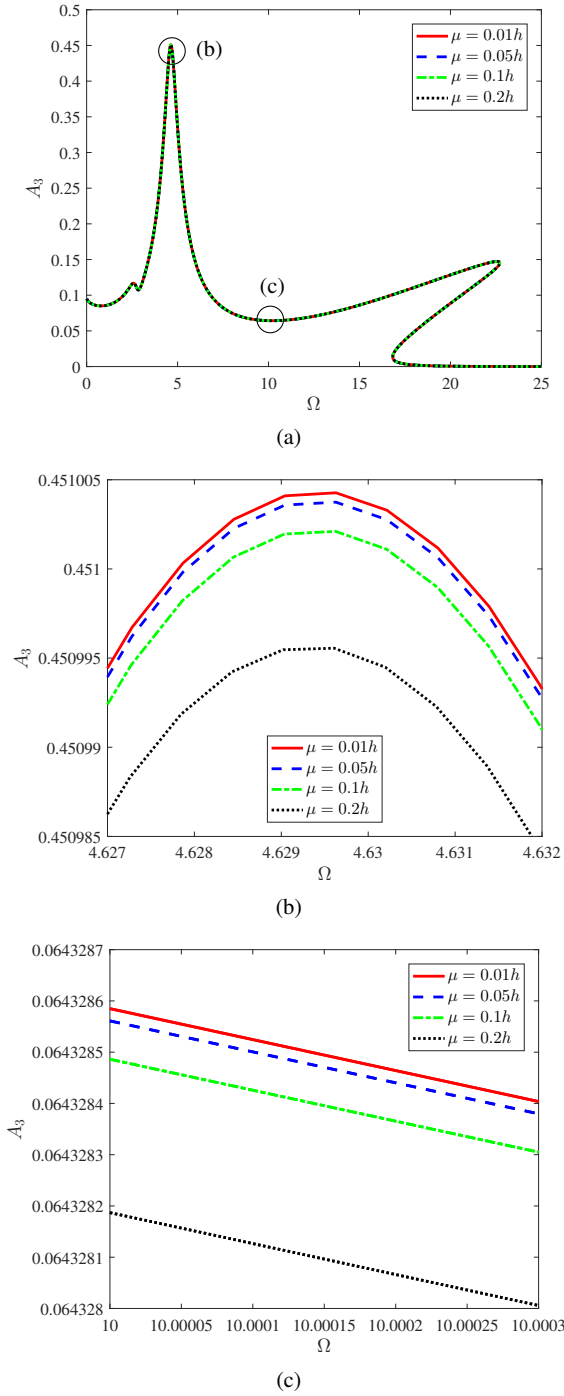
Fig. 8: The amplitude-frequency response curves of the non-linear nonlocal strain gradient FG beam on a fractional visco-Pasternak foundation for the third harmonic amplitude A_3 for different values of the nonlocal parameter μ, sub-figure (a). The periodic response obtained by the incremental harmonic balance (IHB) method is taken close to the resonant state in sub-figure (b) and far from the resonant state in sub-figure (c).

$s_0 - s_5$ are calculated as

$$\{s_0, s_1, s_2, s_3, s_4, s_5\} = \int_0^1 \{\phi, \phi^2, \phi''\phi, \phi^{IV}\phi, \phi^{VI}\phi, \phi'^2\} d\overline{X}. \tag{45}$$

By replacing Eq.(44) into Eq.(43), and using Eq.(45) we obtain the following nonlinear fractional-order differential equation

$$\ddot{q} + \gamma D_\tau^\alpha q + \omega_0^2 q + \theta q^3 = f_0 + f_1 \cos\Omega\tau, \tag{46}$$

where parameters are given as

$$\gamma = \frac{K_1 s_1 - K_2 s_2 - \lambda^2 K_1 s_2 + \lambda^2 K_2 s_3}{s_1 - y s_2 - \lambda^2 s_2 + y\lambda^2 s_3},$$
$$\omega_0^2 = \frac{k_1 s_1 - k_2 s_2 - \lambda^2 k_1 s_2 + \lambda^2 k_2 s_3 + s_3 - \Sigma^2 s_4}{s_1 - y s_2 - \lambda^2 s_2 + y\lambda^2 s_3},$$
$$\theta = \frac{-\frac{1}{2} s_5 s_2 + \frac{1}{2} s_5 s_3 \lambda^2}{s_1 - y s_2 - \lambda^2 s_2 + y\lambda^2 s_3}, \tag{47}$$
$$f_0 = \frac{-s_0 F_0}{s_1 - y s_2 - \lambda^2 s_2 + y\lambda^2 s_3},$$
$$f_1 = \frac{-s_0 F_1}{s_1 - y s_2 - \lambda^2 s_2 + y\lambda^2 s_3}.$$

Note that Eq.(40) could have been nondimensionalized in many ways. Among them, the optimal one is given in this paper. Radius of gyration k_x (Eq.(42)) is introduced in nondimenzionalization process with the purpose to reduce nonlinear parameter θ in Eq.(46). Extreme high values of θ comparing to linear stiffness parameter ω_0^2 would later induce problems with solving fractional-order differential equation of motion (Eq.(46)).

4 Nonlinear periodic response

Analytical perturbation methods such as the multiple scales method are usually used to solve the nonlinear fractional differential equations in the case of weak nonlinearity [55]. For strong nonlinearities, it is more common to use numerical methods such as the differential quadrature method (DQM) [40] or incremental harmonic balance (IHB) method [46]. A brief review of available numerical methods for solving the aforementioned nonlinear fractional differential equations is given by Zhou et al. [74]. In this study, periodic solutions found by the IHB method are verified with the results from both the perturbation multiple scales and Newmark numerical method.

4.1 The incremental harmonic balance method

IHB method has established reference quotations for solving the nonlinear structural problems. Among others, Dou and

(a)

(b)

(c)

(a)

(b)
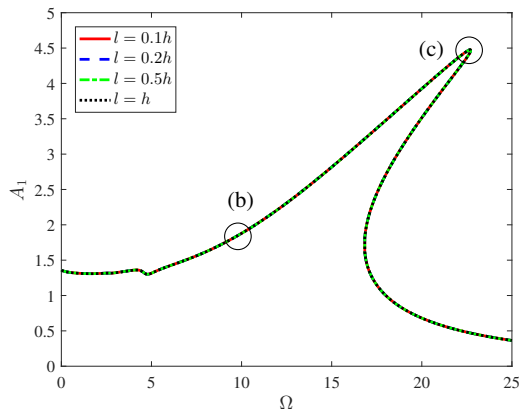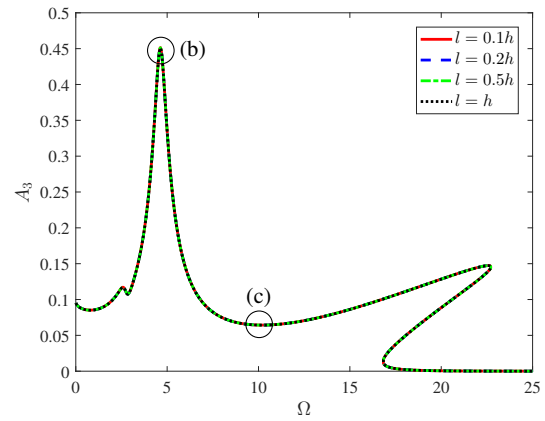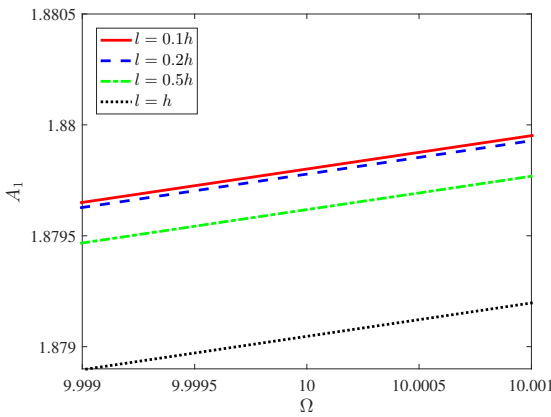
(c)

Fig. 9: The amplitude-frequency response curves of the non-linear nonlocal strain gradient FG beam on a fractional visco-Pasternak foundation in the first harmonic amplitude A_1 and different values of the length scale parameter l are given in sub-figure (a). The periodic response obtained by the IHB method and taken far from the resonant state is given in sub-figure (b) and close to the resonant state in sub-figure (c).

Fig. 10: The amplitude-frequency response curves of the nonlinear nonlocal strain gradient FG beam on a fractional visco-Pasternak foundation in the third harmonic amplitude A_3 for different values of the length scale parameter l are given in sub-figure (a). The periodic response obtained by the IHB method taken close to resonant state is given in sub-figure (b), and far from the resonant state in sub-figure (c).

Jensen [7] developed a method for optimizing the nonlinear structural resonance with time-harmonic loads by using the IHB. Karlicic et al. [25] used IHB and perturbation method of multiple scales for investigation of the dynamic behavior and stability for a single wall carbon nanotube modeled as a nonlinear nanobeam embedded in a Kelvin-Voigt viscoelastic medium. IHB method was also employed for studying the coupled Duffing oscillators [26] and parametrically amplified Mathieu-Duffing oscillator [27] used for energy harvesting purposes.

To apply the IHB method, we introduce a new time scale $\overline{\tau} = \Omega\tau$ into Eq.(46) to obtain the system of nonlinear ordinary differential equations in the following form

$$\Omega^2 \frac{d^2q}{d\overline{\tau}^2} + \gamma\Omega^\alpha D_{\overline{\tau}}^\alpha q + \omega_0^2 q + \theta q^3 = f_0 + f_1\cos\overline{\tau}. \tag{48}$$

For the arbitrarily chosen initial values for q_0 and Ω_0 of the steady-state modal amplitude, a neighboring state of motion has the incremental changes to the current state and can be expressed in the following form

$$q = q_0 + \Delta q, \quad \Omega = \Omega_0 + \Delta\Omega. \tag{49}$$

Substituting Eq.(49) into Eq.(48) and neglecting higher-order terms, we obtain a linearized incremental relation given as

$$\begin{aligned}\Omega^2\Delta q'' &+ \gamma\Omega_0^\alpha D_{\overline{\tau}}^\alpha \Delta q + \omega_0^2\Delta q + 3\theta q_0^2\Delta q \\ &= r - 2\Omega_0 q_0''\Delta\Omega f_0 + f_1\cos\overline{\tau},\end{aligned} \tag{50}$$

where r is residual term given as

$$r = -\left(\Omega_0^2 q_0'' + \gamma\Omega_0^\alpha D_{\overline{\tau}}^\alpha q_0 + \omega_0^2 q_0 + \theta q_0^3\right). \tag{51}$$

To obtain the periodic solutions of the fractional-order differential equation, q_0 and Δq are expanded as a finite Fourier series of N terms as

$$q_0 = a_0 + \sum_{n=1}^N \left[a_n\cos(n\overline{\tau}) + b_n\sin(n\overline{\tau})\right] = CA_0, \tag{52}$$

$$\Delta q = \Delta a_0 + \sum_{n=1}^N \left[\Delta a_n\cos(n\overline{\tau}) + \Delta b_n\sin(n\overline{\tau})\right] = C\Delta A, \tag{53}$$

where

$$C = \begin{bmatrix} 1 & \cos\overline{\tau} & \cos 2\overline{\tau} & ... & \cos N\overline{\tau} & \sin\overline{\tau} & \sin 2\overline{\tau} & ... & \sin N\overline{\tau}\end{bmatrix}, \tag{54}$$

$$A_0 = \begin{bmatrix} a_0 & a_1 & a_2 & ... & a_N & b_1 & b_2 & ... & b_N\end{bmatrix}^T, \tag{55}$$

$$\Delta A = \begin{bmatrix} \Delta a_0 & \Delta a_1 & \Delta a_2 & ... & \Delta a_N & \Delta b_1 & \Delta b_2 & ... & \Delta b_N\end{bmatrix}^T. \tag{56}$$

We substitute Eqs.(52),(53),(54),(55) and (56) into Eq.(50), and apply the Galerkin procedure. Since a fractional-order

derivative is an aperiodic function, in the integration procedure we choose the time period $T = \infty$ and average the integration results for the fractional derivative. In the same way, for the periodic function, we choose the time terminal as $T = 2\pi$, which leads us to the following system of equations

$$\begin{aligned}\frac{1}{2\pi}&\int_0^{2\pi} (\delta\Delta q)^T \left[\Omega^2\Delta q'' + \omega_0^2\Delta q + 3\theta q_0^2\Delta q\right] d\overline{\tau} \\ &+ \frac{1}{T}\int_0^T (\delta\Delta q)^T \left[\gamma\Omega^\alpha D_{\overline{\tau}}^\alpha \Delta q\right] d\overline{\tau} \\ &= \frac{1}{2\pi}\int_0^{2\pi} (\delta\Delta q)^T \left[-\Omega^2 q_0'' - \omega_0^2 q_0 - \theta q_0^3\right. \\ &\qquad \left. + f_0 + f_1\cos\overline{\tau}\right] d\overline{\tau} - \frac{1}{T}\int_0^T (\delta\Delta q)^T \left[\gamma\Omega^\alpha D_{\overline{\tau}}^\alpha q_0\right] d\overline{\tau} \\ &\quad - \frac{1}{2\pi}\int_0^{2\pi} (\delta\Delta q)^T \left[2\Omega_0 q_0''\right] d\overline{\tau}\Delta\Omega.\end{aligned} \tag{57}$$

This gives us a system of linearized algebraic equations in terms of ΔA in the following form

$$M\Delta A + V\Delta\Omega = R, \tag{58}$$

where elements of the Jacobi matrix M, the corrective vector R, and vector V are given in Appendix 1.

In case that we want the solution at a given single frequency, we would set $\Delta\Omega$ to zero in Eq.(58). Otherwise, we would solve Eq.(58) for both A and $\Delta\Omega$, but insert $\Delta\Omega$ in the first entry of the vector ΔA and transform the system of equations. We initialize solution process by entering guessed values of A, and calculate ΔA using Eq.(58). The solution ΔA is then added to the current estimated value of A to determine the new vector A, i.e,

$$A_{k+1} = A_k + \Delta A. \tag{59}$$

We repeat this process until the value of the residuum norm $|R|$ is within preset tolerance (in our case less than 10^{-5}).

4.2 The continuation method

For starting the recurrent continuation process we need to obtain the periodic response in two successive points by using the IHB method. These initial points are usually taken far from the resonant state, where response amplitudes for both of them are having similar and small values. Then we apply the predictor-corrector method to carry out point-to-point computation for determining the corresponding branches of the frequency responses. Eq.(58) can be rewritten in the more general matrix form as

$$\begin{bmatrix} M & V\end{bmatrix}\begin{bmatrix} \Delta A \\ \Delta\Omega\end{bmatrix} = R. \tag{60}$$
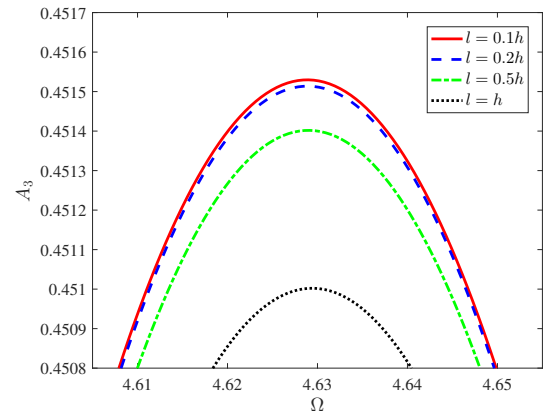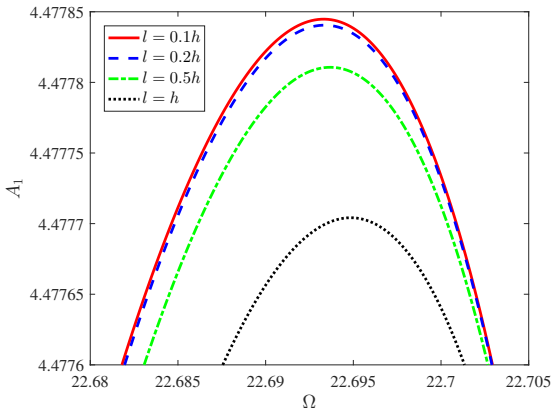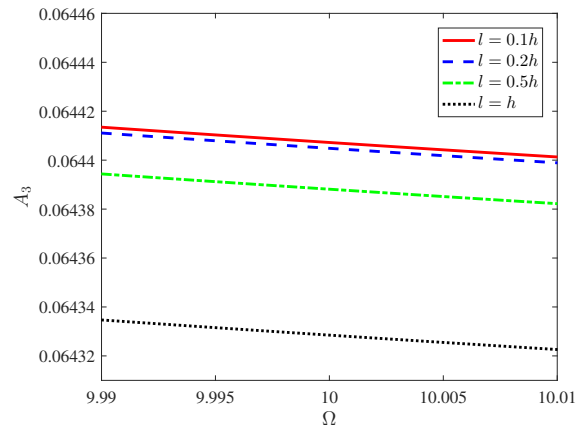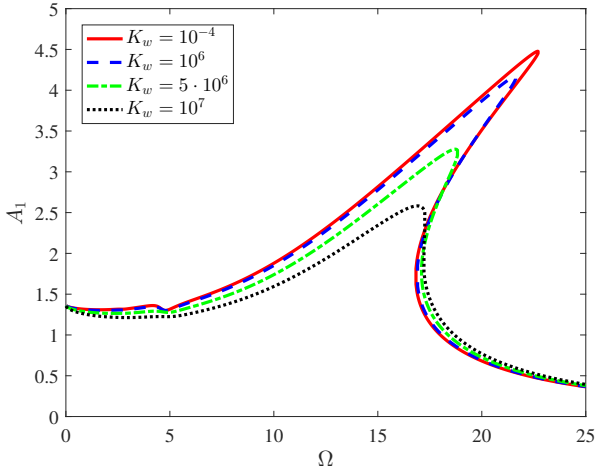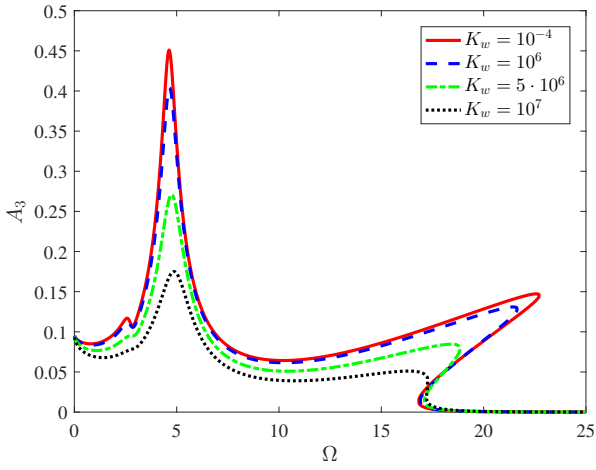
Fig. 11: The amplitude-frequency response curves of the nonlinear nonlocal strain gradient FG beam on a fractional visco-Pasternak foundation. Amplitudes A_1 (a) and A_3 (b) are plotted for different values of the parameter K_w.

Fig. 12: The amplitude-frequency response curves of the nonlinear nonlocal strain gradient FG beam on a fractional visco-Pasternak foundation. Amplitudes A_1 (a) and A_3 (b) are plotted for different values of the parameter k_w.

We introduce new vectors $X = [A \ \ \Omega]^T$ and $\Delta X = [\Delta A \ \ \Delta\Omega]^T$. Let us also introduce a function $g(X)$ of vector X in the following form: Eq.(61). Note that the function $g(X)$ can be defined in many ways, but the one given in Eq.(61) is the most appropriate

$$g(X) = X^T X. \tag{61}$$

We will also introduce arc-length parameter η to follow the direction of the path. An augmented equation would be

$$g(X) - \eta = 0. \tag{62}$$

The slope can be determined by using the two previous known points X_{k-1} and X_{k-2} on the response curves, such as

$$X' = \frac{X_{k-1} - X_{k-2}}{\|X_{k-1} - X_{k-2}\|}. \tag{63}$$
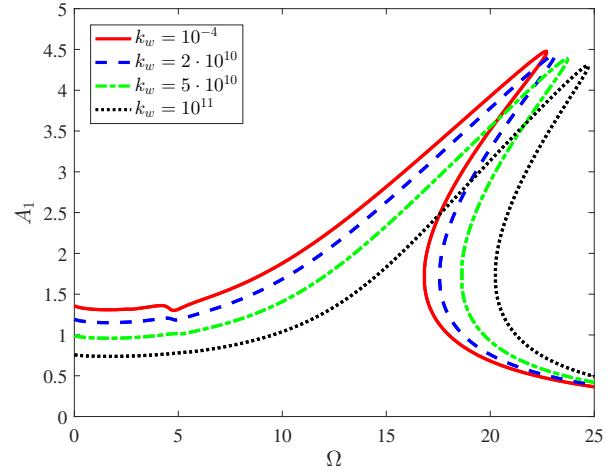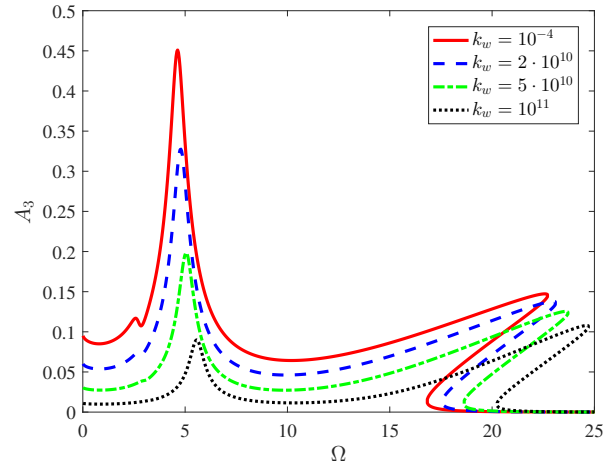
The first prediction of the next point can be determined by

$$X_u = X_{k-1} + \Delta\eta X'. \tag{64}$$

Eq.(60) can be extended with Eq.(62), and then the tangent stiffness matrix and residual vector can be given in the following form

$$\begin{bmatrix} M & V \\ \frac{\partial g}{\partial A} & \frac{\partial g}{\partial \Omega} \end{bmatrix} \begin{bmatrix} \Delta A \\ \Delta\Omega \end{bmatrix} = \begin{bmatrix} R \\ \Delta\eta - g \end{bmatrix}. \tag{65}$$

More information about the continuation method can be found in [10, 5, 64].

5 Numerical results

The methodology outlined in the previous section is utilized herein to find the solution of the fractional-order forced Duffing differential equation Eq.(46) and examine the resonance of a nonlocal FG beam on a fractional visco-Pasternak foundation. The combination of the IHB and path-following methods are introduced to trace branches of periodic solutions of a nonlinear model of a nonlocal strain-gradient beam on a fractional visco-Pasternak foundation with direct transversal harmonic excitation. The obtained diagrams are showing periodic responses given in the form of amplitude-frequency curves. Firstly, beam natural frequency for two different models, obtained by simplifying our model, are verified for the data available in the literature (Tables 1 and 2). In the second part of the numerical study, the validity of the results from the IHB method is examined (Figs.(3,4,6)), which is then followed by the parametric study in the frequency (Figs.(5,7-16)) and time-domain (Fig.(17)). It is demonstrated that the fractional visco-Pasternak layer has a significant influence on the response amplitudes. Moreover, the results obtained by the IHB method are verified with the results from multiple scales and the Newmark method. The last part of the numerical results section is devoted to the analysis of the influence of different parameters on the response. The results revealed the importance of the first and third harmonics. The parameter values of the presented mechanical model are adopted from the paper [30], extended with parameters for fractional Pasternak layer and FG material, and presented in Table 3. The static part of the excitation force Q_0 is set to zero and the dynamic part Q_1 is given in the table. When some parameter is varied remaining coefficients are taken from the Table 3. Moreover, it should be noted that the number of adopted harmonics in the Fourier series is $N = 6$ and this is used in all numerical examples. The amplitudes obtained by the IHB method and corresponding to particular Fourier coefficients (Eq.(55)) and harmonics (Eq.(54)) are computed as given in Eq.(66),

$$A_0 = a_0, \quad A_i = \sqrt{a_i^2 + b_i^2}, \quad (i = 1, 2, \ldots, N). \quad (66)$$

For verification with the multiple scale method, a small non-dimensional bookkeeping parameter takes the value $\varepsilon = 0.01$.

5.1 Verification

To check the derivation of the equation of motion, eigenfrequencies of two simplified models are computed and compared with results obtained by other authors. Table 1 compares the first five non-dimensional fundamental natural frequencies of a local Euler-Bernoulli beam resting on Winkler-Pasternak foundation for the simply supported boundary conditions with foundation parameters $k_1 = 25$, $k_2 = 25$ with

Table 1: The first five non-dimensional fundamental natural frequencies of a local Euler-Bernoulli beam resting on Winkler-Pasternak foundation for the simple-supported boundary conditions ($k_1 = 25, k_2 = 25$)

Present	Ref.[59]	Ref.[13]	Ref.[68]	Ref.[43]
19.2133	19.2133	19.2133	19.21	19.2178
50.7002	50.7002	50.7002	50.7	50.7804
100.6767	100.677	100.6767	100.7	-
170.0281	170.028	170.0281	170.1	-
258.9868	258.987	258.9868	259.1	-

Table 2: Comparison of non-dimensional fundamental natural frequencies of simply supported nonlocal Euler-Bernoulli beam with different nonlocal parameters μ ($L = 10, h = 1, \rho = 1, E = 30 \cdot 10^6, \nu = 0.3$.)

μ	Present	Ref.[52]	Ref. [1]	Ref.[72]
0	9.8293	9.8696	9.8298	9.8696
1	9.3774	9.4159	9.3814	9.4159
2	8.9826	9.0195	8.9892	9.0195
3	8.6338	8.6693	8.6424	8.6693
4	8.3228	8.3569	8.3329	8.3569

Table 3: Parameter values of the presented mechanical model

Parameter	Symbol	Value
Fractional derivative	α	0.5
Young's modulus at top	E_t	390 GPa
Young's modulus at bottom	E_b	210 GPa
Density at top	ρ_t	3960 kg/m^3
Density at bottom	ρ_b	7800 kg/m^3
Power-law index	k	1
Height of the beam	h	100 nm
Width of the beam	b	1 μm
Length of the beam	L	10 μm
Nonlocal parameter	μ	10 nm
Length scale parameter	l	100 nm
Winkler coeff. of viscoelastic layer	k_w	0.0001 m^{-1}
Winkler coeff. of viscoelastic layer	K_w	0.0001 Ns^α/m^3
Pasternak coeff. of viscoelastic layer	k_g	0.0001 m
Pasternak coeff. of viscoelastic layer	K_g	0.0001 Ns^α/m
Amplitude of excitation force	Q_1	0.003 N

values obtained by other authors [59, 13, 68, 43], where fine agreement can be observed. Besides that, we made a comparison of non-dimensional fundamental natural frequencies of simply supported nonlocal Euler beam with different values of nonlocal stress-gradient parameter μ with data available in the literature [52, 1, 72]. Results are in good agreement.

Fig. 13: The amplitude-frequency response curves of the nonlinear nonlocal strain gradient FG beam on a fractional visco-Pasternak foundation. Amplitudes A_1 (a) and A_3 (b) for different values of the parameter K_g.
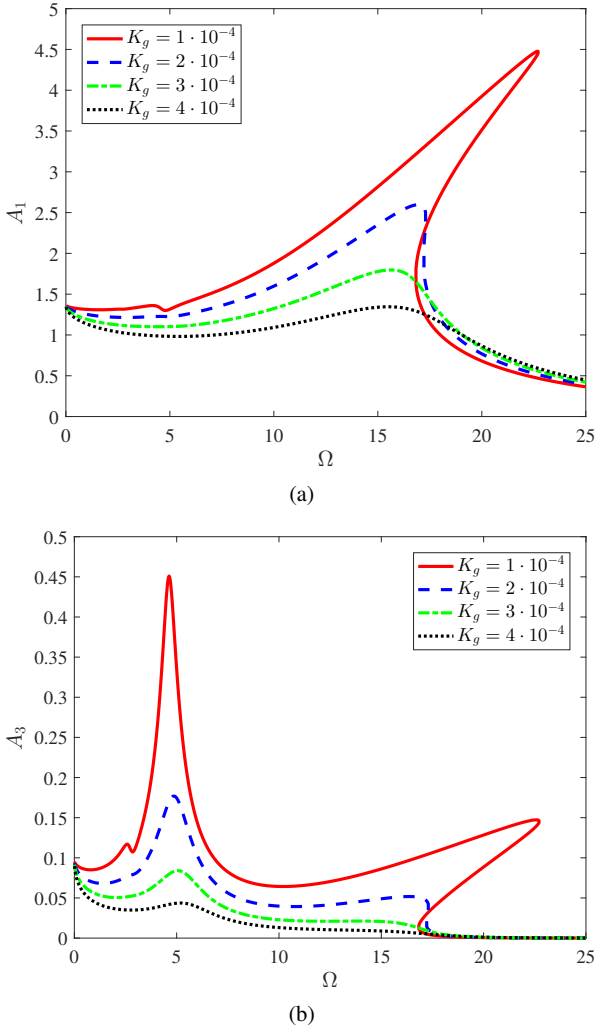

Fig. 14: The amplitude-frequency response curves of the nonlinear nonlocal strain gradient FG beam on a fractional visco-Pasternak foundation. Amplitudes A_1 (a) and A_3 (b) for different values of the parameter k_g.

With the purpose of demonstrating the reliability and accuracy of the proposed approach for the determination of the amplitude-frequency responses and corresponding periodic solutions, the obtained results from the IHB are verified with two different approaches - the perturbation method of multiple scales and the direct numerical integration by using the Newmark method. The first one is used to obtain the amplitude-frequency response diagrams, and the second one to capture periodic motions at desired excitation frequencies. The way we applied the Newmark method to solve the nonlinear fractional differential equation of motion Eq.(48) is given in Appendix 3 thoroughly.

First, we will verify the results by comparing the steady-state frequency responses for the superharmonic resonance case $\Omega = \frac{1}{3}\omega_0$ obtained by the IHB method with the results

from the multiple scales method, as given in Fig.(3) and Fig.(4). In these figures, response amplitudes corresponding to displacement are given on the ordinate axis while excitation frequency Ω is on the abscissa.

In Fig.(3) the amplitude-frequency response curves are given for amplitudes A_3 obtained by the IHB, and amplitudes corresponding to the excitation frequency $\Omega = \frac{1}{3}\omega_0$ obtained by using the multiple scales method. Fractional parametar α is varied. Fig.(3) (b) is zoomed Fig.(3) (a) that enables one to clearly compare the obtained results. Data in Fig.(3) reveals that results obtained by these two methods match well. Besides that, we can also observe that an increase of α decreases the amplitude, which is slightly shifted to the right towards higher frequencies.

In Fig.(4) the frequency response curves are given for amplitudes A_3 obtained by using the IHB method and amplitudes corresponding to the excitation frequency $\Omega = \frac{1}{3}\omega_0$ obtained by using the multiple scales method. External excitation magnitudes are given as: $Q_1 = 0.001$, $Q_1 = 0.002$, and $Q_1 = 0.003$. From this figure, we can observe a good matching between the result obtained by two different methods. Besides that, we can also observe that an increase of the external excitation magnitude increases the amplitude and shift its value to the right towards higher frequencies.

In Fig.(5)(a) and Fig.(5)(b) the frequency response curves are given for the amplitudes A_1 and A_3, respectively, which are given on the ordinate axis while the excitation frequency Ω is on the abscissa. Due to the stiffness-hardening effect of the external excitation force parameter, not only does the maximum amplitude experience a rise but also the frequency response curves are shifted towards higher excitation frequencies. This shifting can be observed for both, the first (Fig.(5) a)) and third harmonic amplitude (Fig.(5) b)). Also, an increase of the external excitation amplitude causes a significant bending of the amplitude-frequency curves so that the multiple-value solutions may exist in the primary resonance case associated with the first and the third harmonic amplitude. Three periodic orbits are selected from the response curves (marked as star points on Fig.(5)), which are then verified with Newmark-based solutions. The periodic solutions are depicted in the phase plane, where the velocity is given on the ordinate axis while the displacement is given on the abscissa, as shown in sub-figures a), b) and c) of Fig.(6). We picked two points close and one far from the resonant state (Fig.(5)). From Fig.(6) we can observe a good matching between the result obtained by the IHB and Newmark method. However, better overlapping is achieved when we are far from the resonant state.

5.2 Parametric study

In the subsequent examples in this chapter, we have shown the influence of different parameters such as nonlocal parameter, strain gradient parameter, power-law index, and parameters of fractional visco-Pasternak foundation on amplitude-frequency response. The influence of excitation force is discussed in the previous subsection.

Fig.(7) and Fig.(8) show the amplitude-frequency response of the nonlinear nonlocal strain gradient FG beam on a fractional visco-Pasternak foundation with external excitation for the first A_1 and the third A_3 harmonic amplitudes, respectively, and different values of the nonlocal parameter μ. In the sub-figures b) and c) are presented magnified parts of the sub-figure a). From the observation of Fig.(7) and Fig.(8), it could be found that variations in the nonlocal parameter are having weak influence in both the first and the third harmonic vibration amplitudes. Due to the large non-linearity
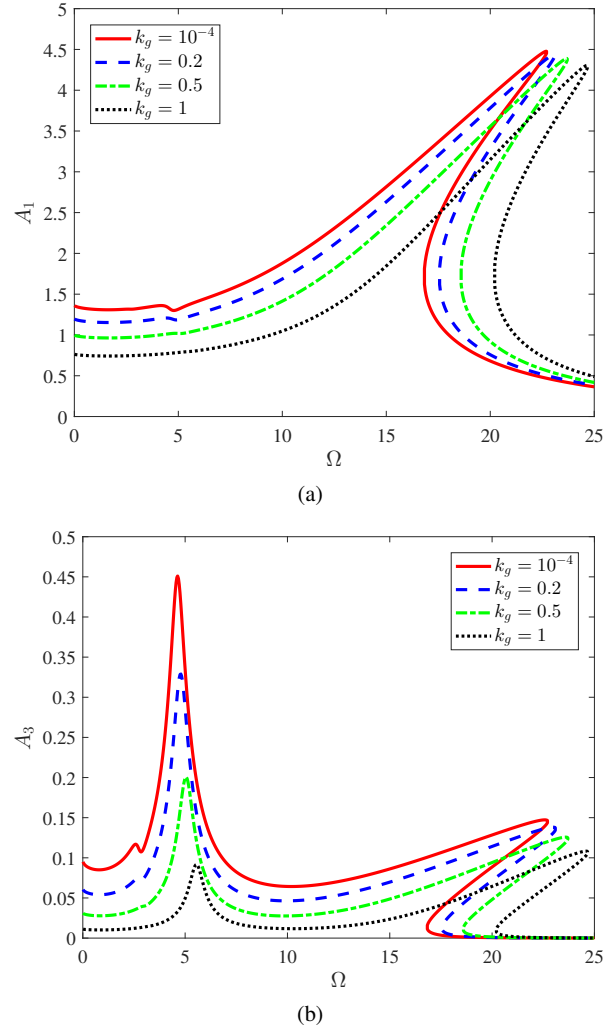

(a)

(b)

Fig. 15: The amplitude-frequency response curves of the nonlinear nonlocal strain gradient FG beam on a fractional visco-Pasternak foundation. Amplitudes A_1 (a) and A_3 (b) for different values of fractional parameter α.

and stiffness of the system, the influence of the nonlocal parameter on amplitude-frequency response is small. In other words, nonlinearity reduces nonlocal parameter influence on the dynamic response of the system.

The amplitude-frequency response curves for different values of the length scale parameter l are given in Fig.(9) and Fig.(10) for the first A_1 and the third A_3 harmonic amplitudes, respectively. In the sub-figures b) and c) are presented magnified parts of the sub-figure a). We observe that variation of the length scale parameter l has a small influence on vibration amplitudes for the primary resonance case and the maximum value. Due to the large non-linearity and stiffness of the system, the influence of the length scale parameter on amplitude-frequency response is small. In other words,
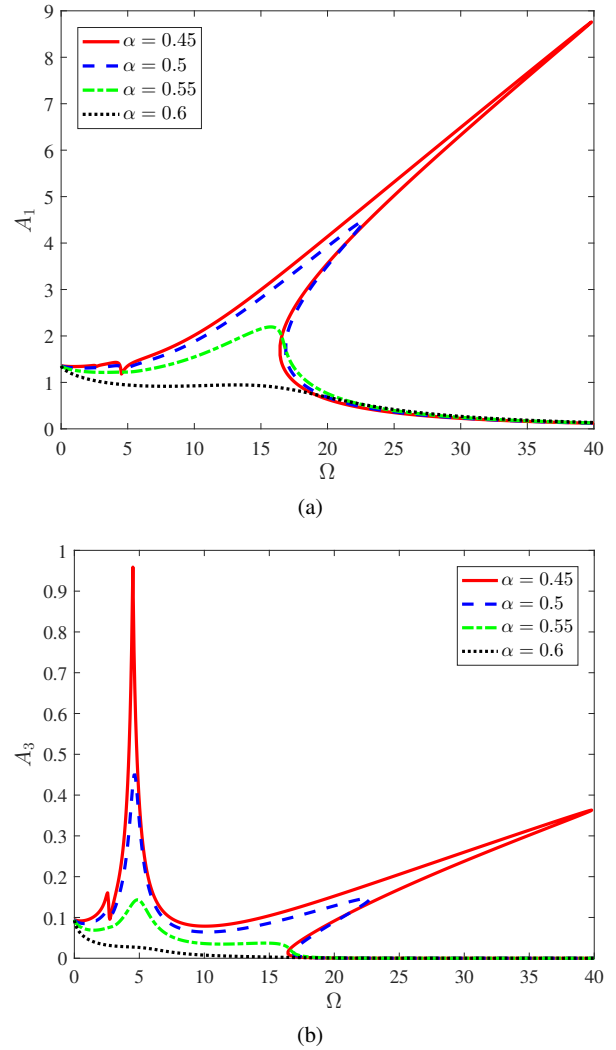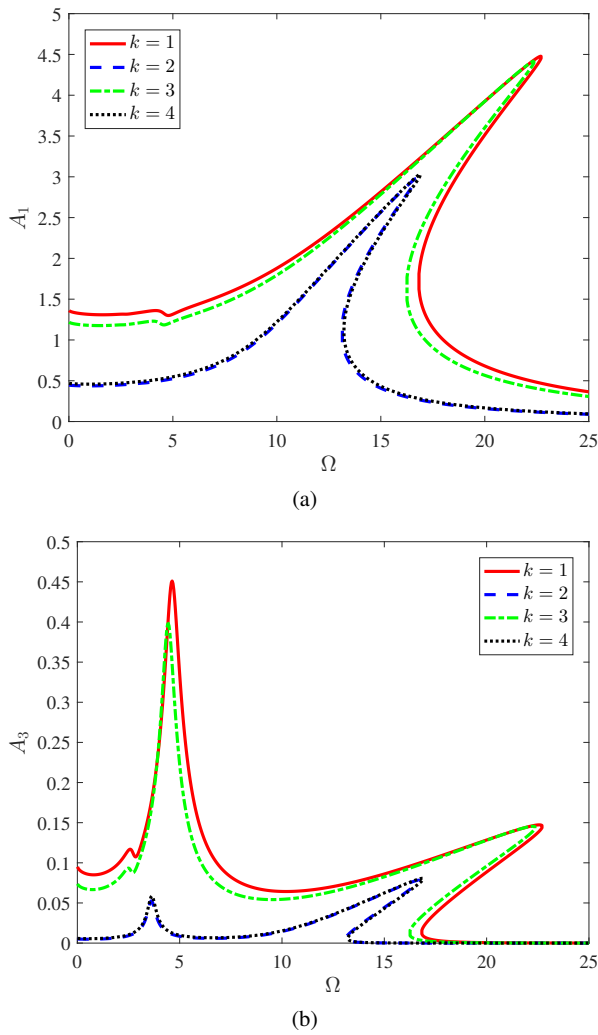
(a)

(b)

Fig. 16: The amplitude-frequency response curves of the nonlinear nonlocal strain gradient FG beam on a fractional visco-Pasternak foundation. Amplitudes A_1 (a) and A_3 (b) for different values of the power-law index k.

nonlinearity reduces length scale parameter influence on the dynamic response of the system.

The amplitude-frequency response curves are given for the first A_1 (Fig.(11) a)) and the third harmonic amplitude A_3 (Fig.(11) b)) and variations of the fractional visco-Pasternak foundation parameter K_w. One can observe that an increase of K_w decreases the amplitude and therefore enlarges the total stiffness of the system. Moreover, an increase of K_w as damping parameter decreases the natural frequencies of the system and therefore the resonance frequency is shifted to the left. Besides that, by looking at the data in-depth, it can be observed that the angle of curve tilt decreases together with the amplitude towards the curvature center for an increase of K_w, which at the same time results in weakening of the hardening type nonlinear behavior.

Fig.(12) shows the amplitude-frequency response curves for the first A_1 (Fig.(12) a)) and the third harmonic amplitude A_3 (Fig.(12) b)) and variations of the foundation parameter k_w. One can observe that an increase of k_w decreases the amplitude with the stabilizing effect to the system vibrations and therefore the total stiffness of the system is enlarged. Besides that, an increase of k_w as a damping parameter decreases the natural frequencies of the system and shifts the resonance frequency to the right.

The amplitude-frequency response curves in the first A_1 (Fig.(13) a)) and the third harmonic amplitude A_3 (Fig.(13) b)) are given for different values of the fractional visco-Pasternak foundation parameter K_g. One can notice that an increase of the parameter K_g decreases the resonance amplitude that is shifted to the left. This indicates that raise of K_g augments the total stiffness of the system. Furthermore, an increase of the parameter K_g causes weakening of the nonlinear hardening behavior of the response. Namely, the hardening-type nonlinearity becomes more apparent when the damping parameter K_g is small.

Fig.(14) shows the amplitude-frequency response curves for the first A_1 (Fig.(14) a)) and the third harmonic amplitude A_3 (Fig.(14) b)) for different values of the foundation parameter k_g. One can notice that an increase of the parameter k_g decreases the resonance amplitude that is shifted to the right significantly enlarging the hardening effects of nonlinearity. This indicates that raise of k_g increases the total stiffness of the system.

By comparing the variation of K_w, k_w, K_g, k_g, one can observe that an increase of the parameter K_g has a bigger influence on the increasing total stiffness of the system than the parameter K_w, even though both parameters contribute to the amplitude decrease. However, k_g and k_w have similar effects of moving the amplitude-frequency curve to the right towards the higher values of the external frequency with the light reduction of amplitude values.

The amplitude-frequency response curves in the first A_1 (Fig.(15) a)) and the third harmonic amplitude A_3 (Fig.(15) b)) are given for different values of the fractional-order derivative α in the model of visco-Pasternak foundation. It can be noticed that a decrease of the fractional-order parameter α by a step of 0,05 increases the amplitude values by almost double in the primary resonance case. This significant influence of the parameter α is caused by damping features of the system become less pronounced due to the elastic-like behavior of the fractional term. Moreover, a decrease of the fractional derivative parameter α makes the equivalent stiffness coefficient larger, which results in the rightwards bending of the amplitude-frequency curves and larger primary resonance frequencies.

Amplitudes of the first A_1 (Fig.(16) a)) and the third harmonic A_3 (Fig.(16) b)) of the amplitude-frequency response are given for different values of the power-law index k that

defines the FG material. One can notice that for $k = 1$ and $k = 3$ the resonant frequencies and hysteresis domain becomes larger and more shifted and bent towards the positive direction of lateral axis than for the case when $k = 2$ and $k = 4$. This can be attributed to increased stiffness properties of the nonlocal beam for these uneven values of the power-law index that increases the hardening nonlinearity and stiffness features of the system.

5.3 Time response

In this section, we show the time responses of the system obtained via the Newmark method. The influences of the fractional-order derivative parameter α (Fig.(17)) are studied to show their effect on the time-dependent behavior of the system. To understand the influence of the fractional visco-Pasternak layer on the initial harmonic excitation of the beam, the following initial conditions are adopted $q(0) = 1$, $\dot{q}(0) = 1$. We adopted the following values of fractional parameter $\alpha = 0.5, 0.6, 0.7$. The dimensionless time period T = 200 is used in the simulation. Similar conclusions can be drawn here as for the amplitude-frequency response. One can observe that an increase of the fractional parameter α leads to stronger damping in time and reduced and attenuated amplitudes of the response. Also, a weak beating phenomenon with decreasing intervals in time can be observed.
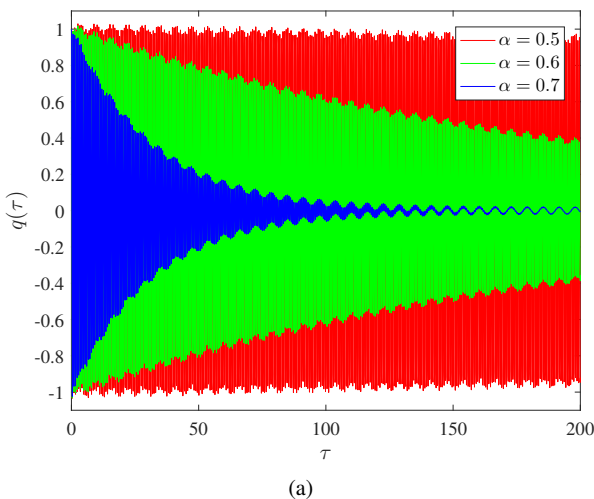

(a)

Fig. 17: The time response curves of the nonlinear nonlocal strain gradient FG beam on a fractional visco-Pasternak foundation. Amplitudes for different values of the fractional derivative parameter.

5.4 Summary of the numerical results

The following conclusions can be drawn about the results presented in this section. The hardening-type nonlinearity becomes more apparent when the force increases and the following parameters decrease: nonlocal parameter μ, strain-gradient length scale parameter l, parameters of visco-Pasternak foundation α, K_w, K_g. If we increase the external excitation amplitude in this system, the primary resonances will be strengthened and shifted rightwards i.e. towards higher excitation frequencies. In this case, the hysteresis domain would also increase. Nonlocal and length scale parameters are both having a small influence on the amplitude-frequency response. Parameters of the visco-Pasternak foundation K_w and K_g augments the total stiffness of the system since their increasing cause response amplitudes decreasing. Specifically, foundation parameters K_w and k_w have smaller influence on amplitude-frequency response comparing to parameters K_g and k_g. The even values of power-law index k causes higher amplitude values in comparison to their odd values.

In addition, we remark on the mutual interactions of the regime in the time domain of the single-amplitude mode of beam vibration. This is observed from the amplitude-frequency diagrams of the first mode A_1, Figs. 7, 9-16, a small jump in amplitude in the region of external frequency about 5, before the resonant region, which corresponds to the contribution of resonant jumps of the third amplitude A_3. The amplitude of the third mode A_3 has a resonant range around this frequency and their values go up to values that can be registered for these small jumps on the amplitude diagrams of the first mode A_1. The second resonant region of the third amplitude A_3 is in the same frequency domain as the one of the first amplitude A_1, the interval $15 - 25$. Thus, the changes of the A_1 diagram from this interval are contributed also by the behavior of the third amplitude A_3 in this interval.

6 Conclusions

In this paper, we analyzed the nonlinear vibration problem of a nonlocal beam resting on the fractional visco-Pasternak foundation by using the nonlocal strain-gradient theory and fractional order damping. The governing equation is derived by using Hamilton's principle and then discretized via the Galerkin approximation, which yields a corresponding nonlinear fractional-order forced Duffing type differential equation. The solution is sought for the steady-state superharmonic resonance conditions by using the perturbation multiple time scales method for the weakly nonlinear case and IHB and Newmark method for the strongly nonlinear case. From the verification study, it is revealed that the IHB method is in good agreement with the multiple time scales analysis

for the weakly nonlinear case and with the numerical Newmark method for the strongly nonlinear case. The main advantage of the IHB method over the multiple scales method lies in the fact that it does not require an introduction of small parameter and thus strong nonlinearity cases can be observed. On the other side, the superiority of the IHB over the Newmark approach is the simple computational implementation and easier determination of periodic solutions. We have also shown that the introduction of the IHB method in the analysis of NLSGT structures can lead to more reliable studies of strongly nonlinear systems. In our parametric study, we concluded that the nonlocal and length scale parameters are having a small influence on the amplitude-frequency response. On the other hand, parameters of the visco-Pasternak foundation remarkably affect the response amplitudes. Finally, the power-law index displays a significant effect on the frequency response, which was also discussed in the numerical analysis. Generally speaking, the system vibration amplitudes are higher for the odd values of the power-law index comparing to materials with the even values of this parameter.

Conflict of interest

The authors declare that they have no conflict of interest.

References

[1] Reza Ansari et al. "A sixth-order compact finite difference method for vibrational analysis of nanobeams embedded in an elastic medium based on nonlocal beam theory". In: *Mathematical and Computer Modelling* 54.11-12 (2011), pp. 2577–2586.

[2] AR Askarian, MR Permoon, and M Shakouri. "Vibration analysis of pipes conveying fluid resting on a fractional Kelvin-Voigt viscoelastic foundation with general boundary conditions". In: *International Journal of Mechanical Sciences* (2020), p. 105702.

[3] Raffaele Barretta et al. "Functionally graded Timoshenko nanobeams: a novel nonlocal gradient formulation". In: *Composites Part B: Engineering* 100 (2016), pp. 208–219.

[4] RC Batra. "Misuse of Eringen's nonlocal elasticity theory for functionally graded materials". In: *International Journal of Engineering Science* 159 (), p. 103425.

[5] Udbhau Bhattiprolu, Anil K Bajaj, and Patricia Davies. "Periodic response predictions of beams on nonlinear and viscoelastic unilateral foundations using incremental harmonic balance method". In: *International Journal of Solids and Structures* 99 (2016), pp. 28–39.

[6] Oreste S Bursi and P-SB SHING. "Evaluation of some implicit time-stepping algorithms for pseudodynamic tests". In: *Earthquake engineering & structural dynamics* 25.4 (1996), pp. 333–355.

[7] Suguang Dou and Jakob Søndergaard Jensen. "Optimization of nonlinear structural resonance using the incremental harmonic balance method". In: *Journal of Sound and Vibration* 334 (2015), pp. 239–254.

[8] Sami El-Borgi, Ralston Fernandes, and JN Reddy. "Non-local free and forced vibrations of graded nanobeams resting on a non-linear elastic foundation". In: *International Journal of Non-Linear Mechanics* 77 (2015), pp. 348–363.

[9] Samir A Emam and Ali H Nayfeh. "Postbuckling and free vibrations of composite beams". In: *Composite Structures* 88.4 (2009), pp. 636–642.

[10] Sebastian Engelnkemper et al. "Continuation for thin film hydrodynamics and related scalar problems". In: *Computational Modelling of Bifurcations and Instabilities in Fluid Dynamics*. Springer, 2019, pp. 459–501.

[11] A Cemal Eringen. "On differential equations of nonlocal elasticity and solutions of screw dislocation and surface waves". In: *Journal of applied physics* 54.9 (1983), pp. 4703–4710.

[12] Georgios I Evangelatos and Pol D Spanos. "An accelerated Newmark scheme for integrating the equation of motion of nonlinear systems comprising restoring elements governed by fractional derivatives". In: *Recent advances in mechanics*. Springer, 2011, pp. 159–177.

[13] Guy Joseph Eyebe et al. "Nonlinear vibration of a nonlocal nanobeam resting on fractional-order viscoelastic Pasternak foundations". In: *Fractal and Fractional* 2.3 (2018), p. 21.

[14] Yin Fan, Yang Xiang, and Hui-Shen Shen. "Nonlinear dynamics of temperature-dependent FG-GRC laminated beams resting on visco-Pasternak foundations". In: *International Journal of Structural Stability and Dynamics* 20.01 (2020), p. 2050012.

[15] Yang Gao, Wanshen Xiao, and Haiping Zhu. "Nonlinear vibration of functionally graded nano-tubes using nonlocal strain gradient theory and a two-steps perturbation method". In: *Struct. Eng. Mech* 69.2 (2019), pp. 205–219.

[16] Majid Ghadiri and S Hamed S Hosseini. "Parametric excitation of pre-stressed graphene sheets under mag-

netic field: nonlinear vibration and dynamic instability". In: *International Journal of Structural Stability and Dynamics* 19.11 (2019), p. 1950135.

[17] Mergen H Ghayesh and Ali Farajpour. "A review on the mechanics of functionally graded nanoscale and microscale structures". In: *International Journal of Engineering Science* 137 (2019), pp. 8–36.

[18] Mohammad Hashemian et al. "Nonlocal dynamic stability analysis of a Timoshenko nanobeam subjected to a sequence of moving nanoparticles considering surface effects". In: *Mechanics of Materials* (2020), p. 103452.

[19] XQ He, S Kitipornchai, and KM Liew. "Resonance analysis of multi-layered graphene sheets used as nanoscale resonators". In: *Nanotechnology* 16.10 (2005), p. 2086.

[20] Elmer S Hung and Stephen D Senturia. "Extending the travel range of analog-tuned electrostatic actuators". In: *Journal of microelectromechanical systems* 8.4 (1999), pp. 497–505.

[21] Ilgar Jafarsadeghi-Pournaki et al. "Size-dependent dynamics of a FG nanobeam near nonlinear resonances induced by heat". In: *Applied Mathematical Modelling* (2020).

[22] MH Jalaei, A Ghorbanpour Arani, and H Nguyen-Xuan. "Investigation of thermal and magnetic field effects on the dynamic instability of FG Timoshenko nanobeam employing nonlocal strain gradient theory". In: *International Journal of Mechanical Sciences* 161 (2019), p. 105043.

[23] G Janevski, N Despenić, and I Pavlović. "Thermal buckling and free vibration of Euler-Bernoulli FG nanobeams based on the higher-order nonlocal strain gradient theory." In: *Archives of Mechanics* 72.2 (2020).

[24] Goran Janevski, Ivan Pavlović, and Nikola Despenić. "Thermal buckling and free vibration of Timoshenko FG nanobeams based on the higher-order nonlocal strain gradient theory". In: *Journal of Mechanics of Materials and Structures* 15.1 (2020), pp. 107–133.

[25] Danilo Karličić et al. "Dynamic stability of single-walled carbon nanotube embedded in a viscoelastic medium under the influence of the axially harmonic load". In: *Composite Structures* 162 (2017), pp. 227–243.

[26] Danilo Karličić et al. "Nonlinear energy harvester with coupled Duffing oscillators". In: *Communications in Nonlinear Science and Numerical Simulation* (2020), p. 105394.

[27] Danilo Karličić et al. "Parametrically amplified Mathieu-Duffing nonlinear energy harvesters". In: *Journal of Sound and Vibration* (2020), p. 115677.

[28] David CC Lam et al. "Experiments and theory in strain gradient elasticity". In: *Journal of the Mechanics and Physics of Solids* 51.8 (2003), pp. 1477–1508.

[29] Roman Lewandowski and Przemysław Wielentejczyk. "Nonlinear vibration of viscoelastic beams described using fractional order derivatives". In: *Journal of Sound and Vibration* 399 (2017), pp. 228–243.

[30] Li Li and Yujin Hu. "Nonlinear bending and free vibration analyses of nonlocal strain gradient beams made of functionally graded material". In: *International Journal of Engineering Science* 107 (2016), pp. 77–97.

[31] Li Li and Yujin Hu. "Wave propagation in fluid-conveying viscoelastic carbon nanotubes based on nonlocal strain gradient theory". In: *Computational materials science* 112 (2016), pp. 282–288.

[32] Li Li, Yujin Hu, and Xiaobai Li. "Longitudinal vibration of size-dependent rods via nonlocal strain gradient theory". In: *International Journal of Mechanical Sciences* 115 (2016), pp. 135–144.

[33] Li Li et al. "Size-dependent effects on critical flow velocity of fluid-conveying microtubes via nonlocal strain gradient theory". In: *Microfluidics and nanofluidics* 20.5 (2016), p. 76.

[34] Xiaobai Li et al. "Bending, buckling and vibration of axially functionally graded beams based on nonlocal strain gradient theory". In: *Composite Structures* 165 (2017), pp. 250–265.

[35] Xiaodong Li et al. "Mechanical characterization of micro/nanoscale structures for MEMS/NEMS applications using nanoindentation techniques". In: *Ultramicroscopy* 97.1-4 (2003), pp. 481–494.

[36] CW Lim, G Zhang, and JN Reddy. "A higher-order nonlocal elasticity and strain gradient theory and its applications in wave propagation". In: *Journal of the Mechanics and Physics of Solids* 78 (2015), pp. 298–313.

[37] Hu Liu, Zheng Lv, and Han Wu. "Nonlinear free vibration of geometrically imperfect functionally graded sandwich nanobeams based on nonlocal strain gradient theory". In: *Composite Structures* 214 (2019), pp. 47–61.

[38] Rasheedat M Mahamood et al. "Functionally graded material: an overview". In: (2012).

[39] Fahimeh Mehralian, Yaghoub Tadi Beni, and Mehran Karimi Zeverdejani. "Calibration of nonlocal strain gradient shell model for buckling analysis of nanotubes using molecular dynamics simulations". In: *Physica B: Condensed Matter* 521 (2017), pp. 102–111.

[40] Salwa A Mohamed. "A fractional differential quadrature method for fractional differential equations and fractional eigenvalue problems". In: *Mathematical Methods in the Applied Sciences* (2020).

[41] Meisam Moory-Shirbani et al. "Experimental and mathematical analysis of a piezoelectrically actuated multilayered imperfect microbeam subjected to applied

electric potential". In: *Composite Structures* 184 (2018), pp. 950–960.

[42] Yves Moser and Martin AM Gijs. "Miniaturized flexible temperature sensor". In: *Journal of Microelectromechanical Systems* 16.6 (2007), pp. 1349–1354.

[43] KB Mustapha and ZW Zhong. "Free transverse vibration of an axially loaded non-prismatic single-walled carbon nanotube embedded in a two-parameter elastic medium". In: *Computational Materials Science* 50.2 (2010), pp. 742–751.

[44] Fehmi Najar et al. "Dynamics and global stability of beam-based electrostatic microactuators". In: *Journal of Vibration and Control* 16.5 (2010), pp. 721–748.

[45] Ali H Nayfeh and Walter Lacarbonara. "On the discretization of distributed-parameter systems with quadratic and cubic nonlinearities". In: *Nonlinear Dynamics* 13.3 (1997), pp. 203–220.

[46] Nikola Nešić et al. "Nonlinear superharmonic resonance analysis of a nonlocal beam on a fractional visco-Pasternak foundation". In: *Proceedings of the Institution of Mechanical Engineers, Part C: Journal of Mechanical Engineering Science* (2020), p. 0954406220936322.

[47] Ivan R Pavlović et al. "Dynamic behavior of two elastically connected nanobeams under a white noise process". In: *Facta Universitatis, Series: Mechanical Engineering* 18.2 (2020), pp. 219–227.

[48] John Peddieson, George R Buchanan, and Richard P McNitt. "Application of nonlocal continuum models to nanotechnology". In: *International journal of engineering science* 41.3-5 (2003), pp. 305–312.

[49] Igor Podlubny. *Fractional differential equations: an introduction to fractional derivatives, fractional differential equations, to methods of their solution and some of their applications*. Elsevier, 1998.

[50] SC Pradhan and JK Phadikar. "Nonlocal elasticity theory for vibration of nanoplates". In: *Journal of Sound and Vibration* 325.1-2 (2009), pp. 206–223.

[51] Venkatanarayanan Ramakrishnan and Brian F Feeny. "Resonances of a forced Mathieu equation with reference to wind turbine blades". In: *Journal of vibration and acoustics* 134.6 (2012).

[52] JN Reddy. "Nonlocal theories for bending, buckling and vibration of beams". In: *International journal of engineering science* 45.2-8 (2007), pp. 288–307.

[53] Shahab Saffari, Mohammad Hashemian, and Davood Toghraie. "Dynamic stability of functionally graded nanobeam based on nonlocal Timoshenko theory considering surface effects". In: *Physica B: Condensed Matter* 520 (2017), pp. 97–105.

[54] H Salehipour, AR Shahidi, and H Nahvi. "Modified nonlocal elasticity theory for functionally graded materials". In: *International Journal of Engineering Science* 90 (2015), pp. 44–57.

[55] Marina V Shitikova. "The fractional derivative expansion method in nonlinear dynamic analysis of structures". In: *Nonlinear Dynamics* 99.1 (2020), pp. 109–122.

[56] Mesut Şimşek. "Nonlinear free vibration of a functionally graded nanobeam using nonlocal strain gradient theory and a novel Hamiltonian approach". In: *International Journal of Engineering Science* 105 (2016), pp. 12–27.

[57] Pezhman Sourani et al. "A comparison of the Bolotin and incremental harmonic balance methods in the dynamic stability analysis of an Euler–Bernoulli nanobeam based on the nonlocal strain gradient theory and surface effects". In: *Mechanics of Materials* (2020), p. 103403.

[58] G Sales Teodoro, JA Tenreiro Machado, and E Capelas De Oliveira. "A review of definitions of fractional derivatives and other operators". In: *Journal of Computational Physics* 388 (2019), pp. 195–208.

[59] Necla Togun and Süleyman Murat Bağdatlı. "Nonlinear vibration of a nanobeam on a Pasternak elastic foundation based on non-local Euler-Bernoulli beam theory". In: *Mathematical and Computational Applications* 21.1 (2016), p. 3.

[60] Hoang Lan Ton-That. "A new C0 third-order shear deformation theory for the nonlinear free vibration analysis of stiffened functionally graded plates". In: *Facta Universitatis, Series: Mechanical Engineering* 19.2 (2021), pp. 285–305.

[61] M Trabelssi, S El-Borgi, and MI Friswell. "A high-order FEM formulation for free and forced vibration analysis of a nonlocal nonlinear graded Timoshenko nanobeam based on the weak form quadrature element method". In: *Archive of Applied Mechanics* (2020), pp. 1–24.

[62] Gang-Feng Wang and Xi-Qiao Feng. "Effects of surface elasticity and residual surface tension on the natural frequency of microbeams". In: *Applied physics letters* 90.23 (2007), p. 231904.

[63] Jing Wang and Huoming Shen. "Nonlinear vibrations of axially moving simply supported viscoelastic nanobeams based on nonlocal strain gradient theory". In: *Journal of Physics: Condensed Matter* 31.48 (2019), p. 485403.

[64] Sheng Wang et al. "Applications of incremental harmonic balance method combined with equivalent piecewise linearization on vibrations of nonlinear stiffness systems". In: *Journal of Sound and Vibration* 441 (2019), pp. 111–125.

[65] Zhong Lin Wang and Wenzhuo Wu. "Nanotechnology-enabled energy harvesting for self-powered micro-/nanosystems". In: *Angewandte Chemie International Edition* 51.47 (2012), pp. 11700–11721.

[66] Shao-Fang Wen et al. "Dynamical analysis of strongly nonlinear fractional-order Mathieu-Duffing equation".

In: *Chaos: An Interdisciplinary Journal of Nonlinear Science* 26.8 (2016), p. 084309.

[67] FACM Yang et al. "Couple stress based strain gradient theory for elasticity". In: *International Journal of Solids and Structures* 39.10 (2002), pp. 2731–2743.

[68] T Yokoyama. "Vibrations and transient responses of Timoshenko beams resting on elastic foundations". In: *Ingenieur-Archiv* 57.2 (1987), pp. 81–90.

[69] Davood Younesian et al. "Elastic and viscoelastic foundations: a review on linear and nonlinear vibration modeling and applications". In: *Nonlinear Dynamics* (2019), pp. 1–43.

[70] Paul M Zavracky et al. "Microswitches and microrelays with a view toward microwave applications". In: *International Journal of RF and Microwave Computer-Aided Engineering: Co-sponsored by the Center for Advanced Manufacturing and Packaging of Microwave, Optical, and Digital Electronics (CAMPmode) at the University of Colorado at Boulder* 9.4 (1999), pp. 338–347.

[71] Guoqi Zhang, Zhiqiang Wu, and Yajie Li. "Nonlinear Dynamic Analysis of Fractional Damped Viscoelastic Beams". In: *Int. J. Struct. Stab. Dyn. 19 (11)(2019)* 1950129 (2019).

[72] X Zhao et al. "Coupled thermoelastic nonlocal forced vibration of an axially moving micro/nano-beam". In: *International Journal of Mechanical Sciences* (2021), p. 106600.

[73] Yaxin Zhen and Lin Zhou. "Wave propagation in fluid-conveying viscoelastic carbon nanotubes under longitudinal magnetic field with thermal and surface effect via nonlocal strain gradient theory". In: *Modern Physics Letters B* 31.08 (2017), p. 1750069.

[74] Yongtao Zhou et al. "Implicit-explicit time integration of nonlinear fractional differential equations". In: *Applied Numerical Mathematics* (2020).

Appendix 1

Elements of the Jacobi matrix $M = M_1 + M_2^\alpha$, the corrective vector $R = R_1 + R_2^\alpha$, and vector $V = V_1 + V_2^\alpha$ are defined as:

$$M_1 = \frac{1}{2\pi} \int_0^{2\pi} \left[\Omega^2 C^T \frac{d^2C}{d\bar\tau^2} + \omega_0^2 C^T C + 3\theta q_0^2 C^T C \right] d\bar\tau, \quad (67)$$

$$M_2^\alpha = \frac{1}{T} \int_0^T C^T \left[\gamma \Omega^\alpha D_{\bar\tau}^\alpha (C) \right] d\bar\tau, \quad (68)$$

$$R_1 = -\frac{1}{2\pi} \int_0^{2\pi} \left[\left(\Omega^2 C^T \frac{d^2C}{d\bar\tau^2} + \omega_0^2 C^T C + \theta q_0^2 C^T C \right) d\bar\tau A_0 \right.$$
$$\left. + f_0 C^T + f_0 \cos\bar\tau C^T \right] d\bar\tau, \quad (69)$$

$$R_2^\alpha = -\frac{1}{T} \int_0^T C^T \left[\gamma \Omega^\alpha D_{\bar\tau}^\alpha (C) \right] d\bar\tau A_0, \quad (70)$$

$$V_1 = \frac{1}{2\pi} \int_0^T \left[2\Omega_0 C^T \frac{d^2C}{d\bar\tau^2} \right] d\bar\tau A_0, \quad (71)$$

$$V_2^\alpha = 0. \quad (72)$$

Within each incremental step, only a set of linear equations Eq.(58) has to be solved to obtain the data for the next stage. By applying the procedure established at [66, 46] elements of the matrix M_2^α, and vectors R_2^α and V_2^α can be expressed as

$$M_2^\alpha = \begin{bmatrix} [M_{11}]^\alpha & [M_{12}]^\alpha \\ [M_{21}]^\alpha & [M_{22}]^\alpha \end{bmatrix}, \quad R_2^\alpha = \begin{bmatrix} R_{10}^\alpha \\ R_1^\alpha \\ R_2^\alpha \end{bmatrix}, \quad V_2^\alpha = \begin{bmatrix} V_{10}^\alpha \\ V_1^\alpha \\ V_2^\alpha \end{bmatrix}. \quad (73)$$

Elements of matrix M_2^α, and vectors R_2^α and V_2^α from Eq.(73) are:

$$[M_{11}]_{ij}^\alpha = \delta_{ij} \gamma \Omega^\alpha \frac{i^\alpha}{2} \cos\left(\frac{\alpha\pi}{2}\right),$$
$$i = 0,1,2,...,N, \quad j = 0,1,2,...,N,$$

$$[M_{12}]_{ij}^\alpha = \delta_{ij} \gamma \Omega^\alpha \frac{i^\alpha}{2} \sin\left(\frac{\alpha\pi}{2}\right),$$
$$i = 0,1,2,...,N, \quad j = 1,2,...,N,$$

$$[M_{21}]_{ij}^\alpha = -\delta_{ij} \gamma \Omega^\alpha \frac{i^\alpha}{2} \sin\left(\frac{\alpha\pi}{2}\right),$$
$$i = 1,2,...,N, \quad j = 0,1,2,...,N, \quad (74)$$

$$[M_{22}]_{ij}^\alpha = \delta_{ij} \gamma \Omega^\alpha \frac{i^\alpha}{2} \cos\left(\frac{\alpha\pi}{2}\right),$$
$$i = 1,2,...,N, \quad j = 1,2,...,N,$$

$$R_{10}^\alpha = 0,$$
$$R_{1i}^\alpha = -\gamma \Omega^\alpha \left[a_i \frac{i^\alpha}{2} \cos\left(\frac{\alpha\pi}{2}\right) + b_i \frac{i^\alpha}{2} \sin\left(\frac{\alpha\pi}{2}\right) \right],$$
$$i = 1,2,...,N, \quad (75)$$
$$R_{2i}^\alpha = -\gamma \Omega^\alpha \left[a_i \frac{i^\alpha}{2} \sin\left(\frac{\alpha\pi}{2}\right) + b_i \frac{i^\alpha}{2} \cos\left(\frac{\alpha\pi}{2}\right) \right],$$
$$i = 1,2,...,N,$$

$$V_{10}^\alpha = 0,$$
$$V_{1i}^\alpha = \gamma \alpha \Omega^{\alpha-1} \left[a_i \frac{i^\alpha}{2} \cos\left(\frac{\alpha\pi}{2}\right) + b_i \frac{i^\alpha}{2} \sin\left(\frac{\alpha\pi}{2}\right) \right],$$
$$i = 1,2,...,N, \quad (76)$$
$$V_{2i}^\alpha = \gamma \alpha \Omega^{\alpha-1} \left[a_i \frac{i^\alpha}{2} \sin\left(\frac{\alpha\pi}{2}\right) + b_i \frac{i^\alpha}{2} \cos\left(\frac{\alpha\pi}{2}\right) \right],$$
$$i = 1,2,...,N,$$

where δ_{ij} is Kronecker delta.

Appendix 2

Multiple scales method

Multiple scales is the analytical perturbation method for constructing approximate solutions of nonlinear differential equations. This method is well established in the literature but it is only valid for small nonlinearities and damping. Therefore, we will use it here only for validation purposes. Eq.(46) is well known as the forced Duffing fractional-order differential equation, which can be expressed in terms of small scale parameter ε as in Eq.(77). Let assume for simplicity $f_0 = 0, f = f_1$.

$$\ddot{q} + \varepsilon\overline{\gamma}D_\tau^\alpha q + \omega_0^2 q + \varepsilon\overline{\theta}q^3 = f\cos\Omega\tau. \quad (77)$$

Here, we introduce new parameters as $\gamma = \varepsilon\overline{\gamma}$ and $\theta = \varepsilon\overline{\theta}$. The small bookkeeping parameter ε is put in front of the fractional and nonlinear terms to have weak damping and weak nonlinearity. Please note that the forcing term in Eq.(77) is of the order one (also known as hard forcing) which will help us to study secondary resonances in the system by using the perturbation analysis of the first order. Forcing of order ε would indicate a primary resonance that is the same as in the Duffing equation [51].

Using the multiple scales method, we will seek the solution of Eq.(77) in the following form:

$$q(T_0, T_1, \varepsilon) = q_0(T_0, T_1) + \varepsilon q_1(T_0, T_1) + \cdots. \quad (78)$$

Here, $T_0 = \tau$ is the fast time scale and $T_1 = \varepsilon\tau$ is the slow time scale. We will analyze the system for superharmonic resonance conditions. Firstly, let us define the time derivatives as

$$\frac{d}{d\tau} = D_0 + \varepsilon D_1 + O(\varepsilon^2), \quad (79)$$

$$\frac{d^2}{d\tau^2} = D_0^2 + 2\varepsilon D_0 D_1 + O(\varepsilon^2), \quad (80)$$

$$D^\alpha = D_{0+}^\alpha - \varepsilon\alpha D_{0+}^{\alpha-1}D_1 + \cdots, \quad (81)$$

where $D_n = \frac{\partial}{\partial T_n}, (n = 0, 1, 2, \dots)$ and $D_{n+}^{\alpha-n} = \frac{\partial^{\alpha-n}}{\partial T_{n+}^{\alpha-n}}, (n = 0, 1, 2, \dots)$ are classical and Riemann-Liouville's fractional derivative for new time scales [55]. For the fractional derivative of the exponential function [55], restricted to the first and second-order approximations, the following relationship will be used:

$$D_{0+}^\alpha \exp^{i\omega\tau} = (i\omega)^\alpha \exp^{i\omega\tau}, \quad (82)$$

where i is the imaginary unit. Substituting Eqs. (78), (79), (80), (81) into Eq.(77) and then extracting coefficients of ε^0 and ε^1 we obtain the following equations

$$\varepsilon^0 : D_0^2 q_0 + \omega_0^2 q_0 = f\cos\Omega\tau, \quad (83)$$

$$\varepsilon^1 : D_0^2 q_1 + \omega_0^2 q_1 = -2D_0 D_1 q_0 - \overline{\gamma}D_{0+}^\alpha q_0 - \overline{\theta}q_0^3. \quad (84)$$

The solution of Eq.(83) is sought in the form

$$q_0 = A(T_1)e^{i\omega_0 T_0} + \Lambda e^{i\Omega T_1} + \overline{A}(T_1)e^{-i\omega_0 T_0} + \Lambda e^{-i\Omega T_1}, \quad (85)$$

where A is a complex function in terms of slow time scale, and Λ is defined as

$$\Lambda = \frac{f}{2(\omega_0^2 - \Omega^2)}. \quad (86)$$

Superharmonic resonance $3\Omega \approx \omega_0$

Since we have only cubic nonlinearity in Eq.(77), we will consider the case when $3\Omega = \omega_0 + \varepsilon\sigma$, where σ is the detuning parameter. By substituting q_0 from Eq.(85) into Eq.(84) and removing the secular terms that grow in time unbounded, i.e the coefficients of $e^{i\omega_0 T_0}$, we obtain the corresponding solvability conditions as

$$-2i\omega_0 A' - \overline{\gamma}A(i\omega_0)^\alpha - \overline{\theta}(3A^2\overline{A} + 6A\Lambda^2 + \Lambda^3 e^{i\sigma T_1}) = 0, \quad (87)$$

where $A' = D_1 A$. Then, we use the polar form $A = \frac{1}{2}ae^{i\varphi}$, where the real valued functions a and φ are the amplitude and phase lag of time response, respectively. By substituting A in Eq.(87) and separation of real and imaginary part we obtain

$$\omega_0 a\varphi' - \frac{1}{2}\overline{\gamma}a\omega_0^\alpha\cos\frac{\alpha\pi}{2} - \frac{3}{8}\overline{\theta}a^3 - 3\overline{\theta}a\Lambda^2 - \overline{\theta}\Lambda^3\cos\zeta = 0, \quad (88)$$

$$\omega_0 a' + \frac{1}{2}\overline{\gamma}a\omega_0^\alpha\sin\frac{\alpha\pi}{2} + \overline{\theta}\Lambda^3\sin\zeta = 0, \quad (89)$$

with $\zeta = \sigma T_1 - \varphi$ denoting the new phase angle. Then, we utilize steady-state conditions $a' = 0$, $\zeta' = 0$ in Eq.(88) and Eq.(89), which leads to the relationship between the response amplitude and the detuning parameter in the following form

$$\frac{\overline{\theta}\Lambda^3}{\omega_0 a}\cos\zeta = \sigma - \frac{1}{2}\overline{\gamma}\omega_0^{\alpha-1}\cos\frac{\alpha\pi}{2} - \frac{3}{8}\frac{\overline{\theta}a^2}{\omega_0} - 3\frac{\overline{\theta}\Lambda^2}{\omega_0}, \quad (90)$$

$$\frac{\overline{\theta}\Lambda^3}{\omega_0 a}\sin\zeta = -\frac{1}{2}\overline{\gamma}\omega_0^{\alpha-1}\sin\frac{\alpha\pi}{2}. \quad (91)$$

After simple algebra transformations over Eq.(90) and Eq.(91) following polynomial equation can be obtained

$$\sigma^2 - 2\sigma K + M = 0, \quad (92)$$

with K and M given as

$$K = \frac{1}{2}\overline{\gamma}\omega_0^{\alpha-1}\cos\frac{\alpha\pi}{2} + \frac{3}{8}\frac{\overline{\theta}a^2}{\omega_0} - 3\frac{\overline{\theta}\Lambda^2}{\omega_0}, \quad (93)$$

$$M = K^2 + \left(\frac{1}{2}\overline{\gamma}\omega_0^{\alpha-1}\sin\frac{\alpha\pi}{2}\right)^2, \quad (94)$$

$$\sigma_{1,2} = K \pm \sqrt{K^2 - M}. \tag{95}$$

One can notice that all the parameters contribute to the appearance of the superharmonic resonance of order 1/3 i.e. we have interaction of terms of fractional-order, nonlinear, and external excitation.

Appendix 3

Newmark method

We use Grunwald-Letnikov representation of fractional derivative and apply the Newmark-Beta method for numerical integration. We use two different meshes, coarse mesh for time integration and fine mesh for fractional derivative approximation. Grunwald-Letnikov representation of a fractional derivative of a function $q(\overline{\tau})$ at a point of time $\overline{\tau}$ is

$$_{GL}D_{0,\overline{\tau}}^{\alpha} q(\overline{\tau}) = \lim_{h \to 0} h^{-\alpha} \sum_{k=0}^{n} GL_k q(\overline{\tau} - kh), \tag{96}$$

where

$$GL_k = (-1)^k \binom{\alpha}{k} \tag{97}$$

Grunwald-Letnikov coefficients can also be represented in recursive form as

$$GL_{k=0} = 1, \qquad GL_k = \frac{k - \alpha - 1}{k} GL_{k-1}. \tag{98}$$

Let us define

$$\frac{\Delta\overline{\tau}}{h} = p = 5 \div 20. \tag{99}$$

where $\Delta\overline{\tau}$ is time step for coarse mesh, and h is time step for fine mesh.

Representation of fractional derivative given by Eq.(96) in fine mesh is

$$q_i^{(\alpha)} = h^{-\alpha} \begin{bmatrix} GL_0 \ GL_1 \ \cdots \ GL_{kjp} \end{bmatrix} \begin{bmatrix} q_i \\ q_{i-1} \\ \vdots \\ q_{i-p} \\ q_{i-p-1} \\ \vdots \\ q_{i-2p} \\ q_{i-2p-1} \\ \vdots \\ q_{kjp} \end{bmatrix}, \tag{100}$$

where:

p is the number of past terms of length h in a time integration step of length $\Delta\overline{\tau}$,

j are previous time steps of length $\Delta\overline{\tau}$ that can be approximated accurately by a backward Taylor expansion using the displacement, velocity, and acceleration at a certain time step i,

k represents overall chunks of j time steps that must be taken into consideration to accurately approximate the fractional derivative at a given point.

Taylor backward expansion for the last jp time steps can be represented as in Eq.(101),

$$q_{i-1} = q_i - h\dot{q}_i + \frac{h^2}{2}\ddot{q}_i + O(h^3),$$

$$q_{i-2} = q_i - 2h\dot{q}_i + \frac{4h^2}{2}\ddot{q}_i + O(h^3),$$

$$q_{i-3} = q_i - 3h\dot{q}_i + \frac{9h^2}{2}\ddot{q}_i + O(h^3), \tag{101}$$

$$\vdots$$

$$q_{i-jp} = q_i - jph\dot{q}_i + \frac{j^2 p^2 h^2}{2}\ddot{q}_i + O(h^3),$$

where q_i, $\dot{q}_i$ and $\ddot{q}_i$ are displacement, velocity and acceleration, respectfully, at time step i.

Lets neglect higher order terms. Eq.(101) can be written in the matrix form as Eq.(102),

$$\begin{bmatrix} q_i \\ q_{i-1} \\ q_{i-2} \\ q_{i-3} \\ \vdots \\ q_{i-(jp-1)} \end{bmatrix} = \begin{bmatrix} 1 & 0 & 0 \\ 1 & -h & \frac{h^2}{2} \\ 1 & -2h & \frac{4h^2}{2} \\ 1 & -3h & \frac{9h^2}{2} \\ \vdots & \vdots & \vdots \\ 1 & -(jp-1)h & \frac{(jp-1)^2 h^2}{2} \end{bmatrix} \begin{bmatrix} q_i \\ \dot{q}_i \\ \ddot{q}_i \end{bmatrix} \tag{102}$$

$$= [H_0] \begin{bmatrix} q_i \\ \dot{q}_i \\ \ddot{q}_i \end{bmatrix}.$$

By analogy, the displacements from the step $i-jp$ to the $i-(2jp-1)$ in matrix form in terms of displacements, velocity and acceleration of the $i-jp$ is given by the Eq.(103),

$$\begin{bmatrix} q_{i-jp} \\ q_{i-jp-1} \\ q_{i-jp-2} \\ q_{i-jp-3} \\ \vdots \\ q_{i-(2jp-1)} \end{bmatrix} = \begin{bmatrix} 1 & 0 & 0 \\ 1 & -h & \frac{h^2}{2} \\ 1 & -2h & \frac{4h^2}{2} \\ 1 & -3h & \frac{9h^2}{2} \\ \vdots & \vdots & \vdots \\ 1 & -(jp-1)h & \frac{(jp-1)^2 h^2}{2} \end{bmatrix} \begin{bmatrix} q_{i-j} \\ \dot{q}_{i-j} \\ \ddot{q}_{i-j} \end{bmatrix}$$

$$= [H] \begin{bmatrix} q_{i-j} \\ \dot{q}_{i-j} \\ \ddot{q}_{i-j} \end{bmatrix}.$$

$$\tag{103}$$

Here could jerk also be included, but we didn't do this. Since we omitted jerk, $[H] = [H_0]$. Substituting Eq.(101), Eq.(102) and Eq.(103) in Eq.(100) we obtain following expressions:

$$
q_i^{(\alpha)} = h^{-\alpha} \begin{bmatrix} GL_0 \ GL_1 \ \cdots \ GL_{jp-1} \end{bmatrix} [H_0] \begin{bmatrix} q_i \\ \dot{q}_i \\ \ddot{q}_i \end{bmatrix}
$$
$$
+ h^{-\alpha} \begin{bmatrix} GL_{jp} \ GL_{jp+1} \ \cdots \ GL_{2jp-1} \end{bmatrix} [H] \begin{bmatrix} q_{i-j} \\ \dot{q}_{i-j} \\ \ddot{q}_{i-j} \end{bmatrix} + \cdots
$$
$$
+ h^{-\alpha} \begin{bmatrix} GL_{(k-1)jp} \ \cdots \ GL_{kjp-1} \end{bmatrix} [H] \begin{bmatrix} q_{i-(k-1)j} \\ \dot{q}_{i-(k-1)j} \\ \ddot{q}_{i-(k-1)j} \end{bmatrix},
$$
(104)

$$
q_i^{(\alpha)} = \begin{bmatrix} D_{01} \ D_{02} \ D_{03} \end{bmatrix} \begin{bmatrix} q_i \\ \dot{q}_i \\ \ddot{q}_i \end{bmatrix} + \begin{bmatrix} D_{11} \ D_{12} \ D_{13} \end{bmatrix} \begin{bmatrix} q_{i-j} \\ \dot{q}_{i-j} \\ \ddot{q}_{i-j} \end{bmatrix}
$$
$$
+ \cdots + \begin{bmatrix} D_{(k-1)1} \ D_{(k-1)2} \ D_{(k-1)3} \end{bmatrix} \begin{bmatrix} q_{i-(k-1)j} \\ \dot{q}_{i-(k-1)j} \\ \ddot{q}_{i-(k-1)j} \end{bmatrix},
$$
(105)

$$
\Delta q_i^{(\alpha)} = \begin{bmatrix} D_{01} \ D_{02} \ D_{03} \end{bmatrix} \begin{bmatrix} \Delta q_i \\ \Delta \dot{q}_i \\ \Delta \ddot{q}_i \end{bmatrix} + \begin{bmatrix} D_{11} \ D_{12} \ D_{13} \end{bmatrix} \begin{bmatrix} \Delta q_{i-j} \\ \Delta \dot{q}_{i-j} \\ \Delta \ddot{q}_{i-j} \end{bmatrix}
$$
$$
+ \cdots + \begin{bmatrix} D_{(k-1)1} \ D_{(k-1)2} \ D_{(k-1)3} \end{bmatrix} \begin{bmatrix} \Delta q_{i-(k-1)j} \\ \Delta \dot{q}_{i-(k-1)j} \\ \Delta \ddot{q}_{i-(k-1)j} \end{bmatrix}.
$$
(106)

Lets consider equation of motion Eq.(48) in two consecutive time instants:

$$
\Omega^2 \Delta \ddot{q}_i + \omega_0^2 \Delta q_i + \theta (\Delta q_i)^3
$$
$$
+ \gamma \Omega^\alpha \left({}_{GL}D_{0,\overline{\tau}_i}^\alpha q_i - {}_{GL}D_{0,\overline{\tau}_{i-1}}^\alpha q_{i-1} \right) = f_0 + \Delta f_i,
$$
(107)

where

$$
\Delta f_i = f_1 \cos \overline{\tau}_i.
$$
(108)

By substituting Eq.(106) in Eq.(107) we obtain

$$
\left(\Omega^2 + \gamma \Omega^\alpha D_{03} \right) \Delta \ddot{q}_i + \gamma \Omega^\alpha D_{02} \Delta \dot{q}_i + \left(\omega_0^2 + \gamma \Omega^\alpha D_{01} \right) \Delta q_i
$$
$$
+ \theta (\Delta q_i)^3 = f_0 + \Delta f_i - \Delta f_{correction},
$$
(109)

where

$$
\Delta f_{correction} = \gamma \Omega^\alpha \begin{bmatrix} D_{11} \ D_{12} \ D_{13} \end{bmatrix} \begin{bmatrix} \Delta q_{i-j} \\ \Delta \dot{q}_{i-j} \\ \Delta \ddot{q}_{i-j} \end{bmatrix} + \cdots +
$$
$$
\gamma \Omega^\alpha \begin{bmatrix} D_{(k-1)1} \ D_{(k-1)2} \ D_{(k-1)3} \end{bmatrix} \begin{bmatrix} \Delta q_{i-(k-1)j} \\ \Delta \dot{q}_{i-(k-1)j} \\ \Delta \ddot{q}_{i-(k-1)j} \end{bmatrix}.
$$
(110)

Note that in case of $\Delta f_i = const$, Eq.(109) can be solved using Runge-Kutta method (function ode45 in Matlab). If this is not the case, Eq.(109) can be solved using Newmark-Beta method.

For validation of the IHB solution, the Newmark-Beta method for nonlinear systems is used and implemented according to the procedure presented in [6, 12].